MICROBIAL FIELD PILOT STUDY

By
R. M. Knapp
M. J. McInerney
D. E. Menzie
J. L. Chisholm

November 1990

Work Performed Under Contract No. DE-FG22-89BC14246

Prepared for
U.S. Department of Energy
Assistant Secretary for Fossil Energy

Edith Allison, Project Manager
Bartlesville Project Office
P.O. Box 1398
Bartlesville, OK 74005

Prepared by
University of Oklahoma
Norman, OK 73019

MASTER

TABLE OF CONTENTS

LIST OF TABLES

LIST OF FIGURES

Abstract

This report covers progress made during the first year of the Microbial Field Pilot Study project. Information on reservoir ecology and characterization, facility and treatment design, core experiments, bacterial mobility, and mathematical modeling are addressed in this report.

To facilitate an understanding of the ecology of the target reservoir analyses of the fluids which support bacteriological growth and the microbiology of the reservoir were performed. The results of the water analysis show significant sulfide concentrations. One uniquely shaped motile bacteria was identified and isolated. Five previous isolates were characterized. Various substrates were compared for their ability to promote bacterial growth in brine samples.

A preliminary design of facilities for the operation of the field pilot test was prepared. In addition, procedures for facilities installation and for injection treatments are described.

The Southeast Vassar Vertz Sand Unit (SEVVSU), the site of the proposed field pilot study, is described physically, historically, and geologically. The fields current status is presented and the ongoing reservoir simulation is discussed.

Core flood experiments conducted during the last year were used to help define possible mechanisms involved in microbial enhanced oil recovery. Two possible mechanisms, relative permeability effects and changes in the capillary number, are discussed and related to four Berea core experiments' results. The experiments were conducted at reservoir temperature using SEVVSU oil, brine, and bacteria. Based on relative permeability and capillary number studies by other investigators, it is concluded that these effects cannot account for all of the oil recovered from some cores.

The movement and activity of bacteria in porous media were investigated by monitoring the growth of bacteria in sandpack cores under no flow conditions. The rate of bacteria advancement through the cores was determined. It was possible to monitor the concentration of cells, substrate, and metabolic products as functions of both time and distance in some cores.

A mathematical model of the MEOR process has been developed. The model is a three phase, seven species, one dimensional model. Finite difference methods are used for solution. Advection terms in balance equations are represented with a third-order upwind differencing scheme to reduce numerical dispersion and oscillations. The model is applied to a batch fermentation example and demonstrates a good match with the experimental data.

1. ECOLOGY OF THE RESERVOIR

Introduction.

A thorough understanding of the ecology of the reservoir is a key step in the implementation of a microbial enhanced oil recovery field pilot. It is critical that the chemical composition of reservoir brines be understood so that compatable organisms and nutrients can be selected. The aqueous phase represents the most important part of the reservoir, since it is in this phase that the nutrients required for growth and metabolism will be transported. The analyses of the fluids will provide baseline data needed to assess the sucess of the pilot.

1.1 Experimental Procedure.

Sampling procedure:

Brine was collected from different sites in the field. The sample sites include the source well, the pump manifold, and wells 1A-1, 1A-7, 1A-9, 7-2, 8-2 and, 8-3 respectively. All samples were taken using sterile techniques. All samples were analyzed within four hours for bacterial numbers. The brine samples were stored at 4^0 C until all analyses had been completed.

Fluid analysis:

Hardness, alkalinity, iron, phosphate, sulfate, sulfide, nitrate, nitrite analyses were performed using Hach chemical kits (Hach chemical Co. 1975). Total dry residues and suspended solids were determined using standard procedures (American Public Health Association, 1985).

Bacterial analysis:

To determine the best nutrient source for the stimulation of indigenous microorganisms, brine samples were amended with various nutrient mixtures. Brine samples were dispensed into serum tubes which were closed with rubber bungs and crimp sealed. Where indicated, molasses, sucrose, glucose, and fructose were added to give a final concentration of 0.2% (wt/vol except for molasses which was added on a vol/vol basis). Ammonium nitrate and sodium sulfate were added to give a final concentration of 0.3% (wt/vol). Sodium lactate and sodium thiosulfate were added to give a final concentration of 0.1% (vol/vol) and 0.2% (wt/vol), respectively. Unamended brine samples served as controls. All manipulations were done anaerobically. Tubes were incubated at 35^0C and routinely checked microscopically and turbidimetrically for growth. Anaerobic

molasses-nitrate using bacteria and sulfate-reducing bacteria were enumerated by three-tube most probable number method using a molasses-nitrate medium (Table 1.1) and API-RST medium (Tanner el al. 1985), respectively.

1.2 Results.
Water analysis:

Chemical analysis of the brines collected from different sites is shown in Table 1.4. All brines were highly saline with total dry residues ranging from about 10%, for the source well, to greater than 19% for the brines collected in the portion of the reservoir that was not waterflooded (well 1A-7). The brines contained high levels of divalent cations particularly calcium, ranging from 1.5 to 2.2 %. The alkalinity in most of the brine samples was also high, indicating that some carbonate was present. Little or no phosphate or nitrite was detected in the brine. However, iron and nitrate were detected. The small amounts of nitrate detected in the brines could have been due to interferences in chemical analysis. The pH of all the brines was close to neutral. Significant amounts of sulfate were detected in some brines (Table 1.5). Small amounts of sulfide were also detected in some wells, especially those in the waterflood region of the reservoir indicating a sulfate reducing activity (1.5).

Bacterial analysis:

Since previous studies showed the presence of indigenous microbial populations that were able to grow readily with simple nutrient additions (Knapp et al. 1989), it was important to determine which nutrient source would best stimulate microbial growth. In the present study brines from several wells were amended with different nutrient mixtures (Table 1.6). Results from these experiments show that molasses alone supported good growth of the indigenous populations. However, the addition of molasses together with ammonium nitrate resulted in the largest increases in the growth of the indigenous microbial populations. In some brines, the addition of either glucose or sucrose with or without ammonium nitrate stimulated growth. The addition of a phosphate source and an additional nitrogen source to brines ammended with individual sugars did not stimulate microbial growth. Thus a complex nutrient source is required for optimal growth of the indigenous populations.

Since previous studies have shown the presence of sulfate reducing activity, brines from different sites were amended with acetate and lactate to detect the

presence of sulfate-reducing bacteria. With the exception of brine from well 8-3, there was no evidence of any microbial growth. In the brine from well 8-3, addition of acetate and lactate stimulated growth. Microscopic examination of this brine led to the identification of an uniquely shaped microorganism. The microorganism was highly motile and varied in size from time to time. Studies are presently underway to characterize this microorganism. Enumeration studies showed that the concentration of anaerobic molasses-nitrate using bacteria were much lower than previously found (Table 1.7). Aerobic and anaerobic heterotrophic bacteria that could grow in plate count broth (Difco, Inc, Detroit, MI) with 15% NaCl were not detected. The concentration of sulfate-reducing bacteria was also low (Table 1.8). Higher numbers of sulfate-reducing bacteria were found in brine from the source well (Table 1.8). The relatively low concentrations of sulfate-reducing bacteria and molasses-nitrate using bacteria detected in the brines could have been a result of the biocide treatment which was initiated a few months earlier. Since the addition of lactate and acetate to the brines collected from the water flodded region of the reservoir did not stimulate the growth of sulfate-reducing bacteria this indicated that these brines lack an essential nutrient which is required for the growth of these bacteria.

Five of the most numerous anaerobic, heterotrophic bacterial isolates which were previously isolated were also characterized (Table 1.9). For convenience sake the isolates were designated TA,WA,QB,SA, AND TTL-30, respectively. All of the isolates were strictly anaerobic and obligately halophilic, requiring at least 9% NaCl for growth. They used a variety of carbohydrate substrates such as glucose, sucrose, maltose, fructose, fucose, mannose, galactose, arabinose, trypticase, peptone, inulin, and yeast extract as energy sources and produced acetic acid and solvents. Some of the other substrates utilized by these isolates include; pyrogallic acid, lactic acid, formate, succinate glycerol, and glucosamine.These isolates grew well in a molasses-nitrate-mineral salts medium containing 15% NaCl (wt/vol). Since all of these bacteria are obligately anaerobic and halophilic, they will not survive outside of the reservoir and do not pose a serious health risk.

1.3 Discussion:

An understanding of the microbial ecology of the reservoir is a key step for the development of a sucessful microbial enhanced oil recovery process. Brine

analysis indicates that the reservoir is a highly saline environment. Previous analysis of brines from the reservoir have indicated the presence of microorganisms which require high concentrations of NaCl for growth. The bacteria use molasses and nitrate and form large amounts of gas and at times polymers. The present study shows that a molasses-ammonium nitrate nutrient mixture would best stimulate the growth of indigenous microorganisms in brines from Southeast Vassar Vertz Sand Unit reservoir. Since microbial populations already exist in the sub-surface, the introduction of organisms will not be necessary. Also, since the organisms isolated from the brines are halophilic and anaerobic, their accidental release into the environment will not create any environmental or health hazards since these bacteria will not grow in freshwater systems.

Jenneman et al (1986) reported that sulfide production can be inhibited by high concentrations of nitrate. Thus, the problem of sulfate reduction due to high concentrations of sulfate detected in the reservoir can be controlled with the addition of nitrate.

1.4 Conclusions:

1. A molasses-ammonium nitrate nutrient mixture would best stimulate the growth of indigenous bacterial populations in Southeast Vassar Vertz Sand Unit reservoir.

2. The ability to utilize a fermentable carbohydrate and the halophilic nature of the isolated microorganisms make them a good choice for microbially enhanced oil recovery processes in hypersaline environments.

REFERENCES

American Public Health Association, American Water Works association and Water Control Polution Control Federation: <u>Standard Methods For the Examination of Water and Wastewater,</u> Sixteenth Edition, American Public Health Association, Washington, DC (1985) 92-100, 856-859.

Hach Chemical Co.: <u>Hach Water and Waste Water Analysis Procedure Manual 3rd</u> Edition, Hach Chemical Co, Ames, IA (1975).

Jenneman, G.E., McInerney, M.J., and Knapp, R.M.: " Effect of Nitrate on Biogenic Sulfide Production, " Appl. Environ. Microbiol. (June. 1986) 1205-1211.

Knapp, R. M., McInerney, M. J., and Menzie, D. E., Raiders, R.A.: "Microbial Field Pilot Study," Final report , DOE/BC/14084-6, National Technical Informational Services, Springfield,VA,(1989).

Raiders, R.A., Knapp, R.M., McInerney, M.J., and Menzie, D.E. : "Microbial Selective Plugging and Enhanced Oil Recovery,"J. Indust. Microbiol., (April.1989), 4, 215-230.

Tanner, R. S., Haack, T.K., Semet, R. F., and Greenley, D. E. : " A Mild Steel Tubular Flow System for Biofilm Monitoring, " Proceedings of the United Kingdom National Academy of Corrosion Engineers Corossion '85, Harrowgate, Uk (1985) 259-269.

Table 1.1 : Chemical composition of Molasses - Nitrate medium.

Component	Concentration (per liter)	
Molasses	5.0	ml
Tanner's Mineral solution[a]	20.0	ml
Tanner's Metal solution[b]	10.0	ml
NaCl	150.0	g
Resazurin	0.001	g
NaHCO$_3$	5.0	g
Cysteine HCl	0.5	g
Na$_2$S.9H$_2$O	0.5	g

[a] Table 1.2
[b] Table 1.3

Table 1.2: Chemical composition of Tanner's mineral solution.

Component	Concentration (g/l)
NaCl	40.0
KCl	5.0
NH$_4$Cl	50.0
KH$_2$PO$_4$	5.0
MgSO$_4$.7H$_2$O	10.0
CaCl$_2$.2H$_2$O	1.0

6

Table 1.3: Chemical composition of Tanner's metal solution.

Component	Concentration (gm/l)
Nitroacetic acid	2.0*
MnSo$_4$.H$_2$O	1.0
Fe(NH$_4$)$_2$(SO$_4$)$_2$.6H$_2$O	0.8
CoCl$_2$.6H$_2$O	0.2
ZnSO$_4$.7H$_2$O	0.2
CuCl$_2$.2H$_2$O	0.02
NiCl$_2$.6H$_2$O	0.02
Na$_2$MoO$_4$.2H$_2$O	0.02
Na$_2$SeO$_3$	0.02
Na$_2$WO$_4$	0.02

* Brought to pH 6.0 before addition of metals.

7

Table 1.4: Fluid analysis of brine samples.

Sample Location	Specific Gravity	Total Dry Residue (mg/ml)	Total Suspended (mg/ml)	Total Hardness (mg/ml)	Calcium Hardness (mg/ml)	Total Alkalinity (mg/ml)	Iron (mg/ml)	Phosphate (mg/ml)	Nitrate (mg/ml)	Nitrite (mg/ml)	pH
SW	1.109	109	1.94	21.6	15.1	30	10	<1	10	<0.2	6.0
PM	1.113	110	1.78	24.9	17.6	84	10	1	5	<0.2	7-7.2
1A-1	1.068	112	2.70	26.2	18.1	169	20	1	5	<0.2	7-7.7
1A-7	1.147	191	2.82	32.6	21.9	66	30	<1	10	<0.2	6.7
1A-9	1.071	113	2.41	26.9	17.7	144	20	1	10	<0.2	6.7
7-2	1.112	113	2.91	29.9	19.2	111	30	1	5	<0.2	6-6.4
8-2	1.046	NA	NA	31.6	21.8	NA	NA	NA	NA	<0.2	NA
8-3	1.124	186	1.90	30.4	22.1	45	25	1	5	<0.2	6.5

[a]Data are averages of samples taken on 4/12/89 and 6/22/89. SW: Source well, PM: Pump manifold, NA: Not available.

Table1.5: Concentrations of sulfate and sulfide in brines.

Sample location	Concentration (mg/L)	
	Sulfate[a]	Sulfide[b]
PM	2850	0.3
1A-1	1425	NA
1A-9	1700	5
7-2	2600	1.0
8-2	NA	<0.1
8-3	1050	<0.1

[a]Sampling date 4/12/89
[b]Sampling date 6/22/89
PM: Pump manifold

Table1.6 : Growth in brine samples using different nutrient additions a.

Additions	Samples location b				
	Well 1A-1	Well 1A-9	Well 7-2	Well 8-2	Well 8-3
Molasses	++	++	++	++	++
Molasses + Nitrate	+++	+++	+++	+++	+++
Sucrose	-	+	-	+	+
Sucrose + Nitrate	-	-	-	++	+
Sucrose + Phosphate+Nitrogen + Nitrate	-	-	-	-	-
Glucose	-	++	-	-	+
Glucose+ Nitrate	-	-	-	-	++
Glucose + Phosphate+Nitrogen + Nitrate	-	-	-	-	-
Fructose	-	-	-	-	-
Fructose+ Nitrate	-	-	-	-	-
Fructose+ Phosphate+Nitrogen + Nitrate	-	-	-	-	-
Lactate	-	-	-	-	+
Lactate + Sulfate	-	-	-	-	-
Lactate + Thiosulfate	-	-	-	-	-
Acetate	-	-	-	-	++
Acetate + Sulfate	-	-	-	-	-
Acetate + Thiosulfate	-	-	-	-	+

aConcentration each in %w/v : 0.2, Molasses;0.2, Sucrose; 0.2, Fructose; 0.2, Glucose; 0.1,Acetate; 0.1, Lactate; 0.3, Nitrate; 0.3, Thiosulfate; 0.2, Sulfate; 0.025, Nitrogen as NH4Cl; 0.07, Phosphate.
b Growth: +++ OD > 0.3; ++ OD 0.1-0.3; + OD 0.1; - No turbidity. Tubes were checked microscopically to verify the presence of microbial cells.

10

Table 1.7: Numbers of Molasses nitrate-using bacteria in brine samples a

Sample location	Most probable number (per ml)
Source well	110
Pump manifold	47
Well 7-2	110
Well 8-3	110
Well 1A-1	4
Well 1A-7	2
Well 1A-9	15

a Samples were collected on July 28 1989. Samples were incubated at 35^0c for 45 days.

Table 1.8: Numbers of sulfate-reducing bacteria in brine samples a

Sample location	Most probable number (per ml)
Source well	110
Pump manifold	21
Well 7-2	46
Well 8-3	15
Well 1A-1	24
Well 1A-7	21
Well 1A-9	9

a Samples were collected on July 28 1989. Samples were incubated at 35^0c for 45 days.

Table 1.9: Physiological properties of halophilic isolates.

Isolates[a]	Characteristics					
	Morphology	Gram reaction (%w/v)	Doubling time (h) utilization[b]	NaCl conc.range from glucose	Carbohydrate	End products
1(TA)	Rod	Negative	7.25	9-18	+	Acetate Butanol Propanol
2(WA)	Cocci	Positive	7.25	9-18	+	Acetate Butanol Propanol
3(QB)	Cocci	Negative	10	6-22	+	Acetate Butanol Propanol
4(SA)	Cocci	Positive	11	6-22	+	Acetate Butanol Propanol
5(TTL-30)	Rod	Positive	10	9-22	+	Acetate Propanol

[a]Isolates were designated TA,WA,QB,SA,and TTL-30 respectively for convenience sake.
[b]Carbohydrate substrate used: Glucose, sucrose, maltose, fructose, fucose, mannose, arabinose, trypticase,galactose, peptone, inulin, yeast extract.

2. Surface Facilities Design

A preliminary design of the facilities for the operation of this field pilot has been developed. The surface facilities will mix the nutrient-brine injection slugs and inject these mixtures and subsequent brine slugs into the formation. Also, facilities will be installed to gather the produced fluids in a central location allowing their separation and storage.

The injection well (7-2) will have a packer run on a 2.5 in. tubing string set immediately above the perforations in the Vertz sandstone. No special completion is expected. No chemicals will be used to reduce or eliminate bacterial growth in the wellbore.

An overall plan of the injection well facility is presented in Figure 2-1. The Mesa triplex pump is the existing injection pump in the field. This pump will provide brine water for mixing nutrient slugs and provide for the injection of brine spacers between slugs of nutrient mixture. The hot oil truck will be used to deliver molasses to the injection site and keep it warm to allow a lower working viscosity. Frac tanks will be used to mix the nutrient slug and hold it prior to injection. The filter system will reduce the particulate matter in the injection fluid. The filter and recirculation pumps will be used to move the liquids between tanks and recirculate (roll) the fluids in the tanks to insure mixing. The Microbial Field Pilot Study (MFPS) triplex pump will be used to inject the nutrient slug into the main injection line to Well 7-2.

Figure 2-2 is a plan for the installation of the injection equipment. Activities read from right to left. The letters in brackets indicate what services need to be on location to accomplish these tasks.

A flow chart for the nutrient treatment injection is given in Figure 2-3. The molasses will be delivered to location in a hot oil truck. (See Figure 2-1.) The circulating liquid will be kept at 140°F so that the molasses will be warm enough to flow

but not hot enough to caramelize. When there is room in the molasses truck for additional fluid, brine will be added to the molasses and the resulting mixture circulated using the recirculation pump. This will quickly reduce the viscosity of the molasses and increase the recovery of the molasses from the hot oil truck. The molasses and brine will be mixed in approximately equal portions in Frac tank 1. The filter pump will be used to circulate (roll) this mixture to insure mixing. During circulation, ammonium nitrate will be added to tank 1. The 50/50 nutrient/brine mixture will then be pumped through a filter to remove particulates larger than those found in the normal injection [formation] brine. The filtered mixture will then be stored in Frac tank 2 until it is pumped using a triplex pump into the main injection line which is simultaneously fed by the field injection pump. The resulting mixture will be 90% brine, 10% nutrient when it arrives at the sandface for injection. An alternative procedure (Figure 2-3) is to prepare a 90/10 mixture in Frac Tank 2 which is injected directly into the formation using the MFPS triplex pump.

Approximately 1000 bbl of the 90/10 mix will be injected over two days with around 600 psig surface pressure. This will be followed by 5 days of brine injection using the field injection pump. The desired rate of injection is 500 bbl per day. The purpose of this procedure is to have the nutrient mixture in the wellbore for as short a period as possible and use the brine flush to distribute the nutrients away from the wellbore and into the reservoir rock to avoid microorganism growth in the wellbore.

Each production well will have a pumping unit (equivalent to a Bethlehem 57D) installed . Three quarter inch sucker rods will be used to lift a 1.5 in. plunger pump. The 2.5 in. tubing will be anchored just above the perforations. The wells will be pumped at rates to maintain a volume balance between injection and withdrawal. Figure 2-4 is a plan for the installation of the production well units. The activities read from right to left. In both injection and production wells a well logging survey will be performed to determine porosity and fluid saturations behind the pipe.

14

Figure 2-5 is a layout of the gathering system design. The flow lines will be 2 in. pipe of steel, fiberglass, or black polyethylene material. Other than the two strings that must be buried due to current land use it may be possibe to run the lines on the surface.

Figure 2-6 shows the separator and tank batteries required for this pilot. A simple "gunbarrel separator" will be used to separate the oil and produced water. One oil tank and two water tanks will be used to store the produced fluids. The oil will be sold by the field operator. We expect all of the produced water to be reinjected into the reservoir.
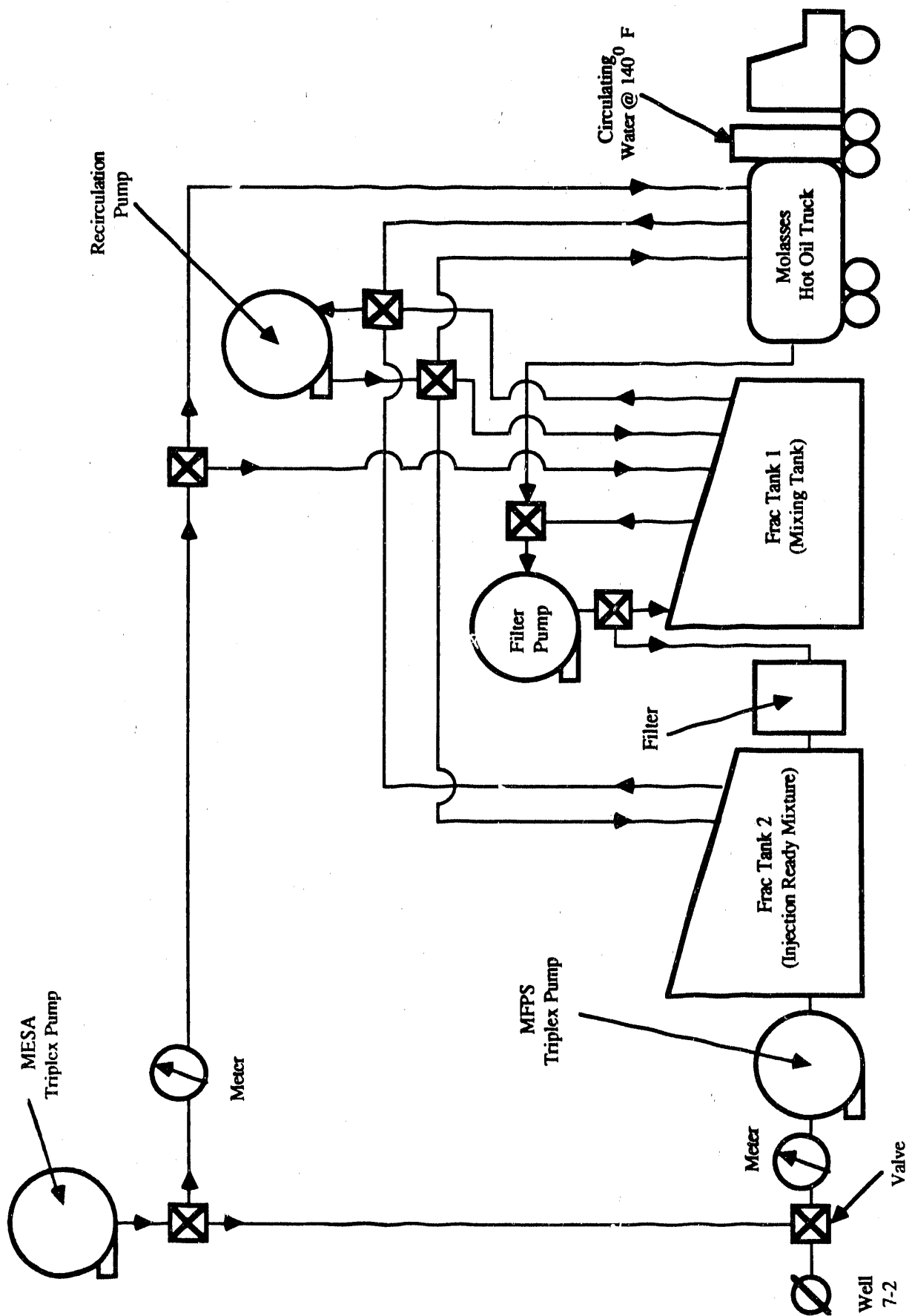
Figure 2-1 Injection Well Facility

INJECTION WELL INSTALLATION

Build pads [G]

Improve location [G]
and roads
(if necessary)

Pull and inspect [C]
tubing and packer
(replace if necessary)

Wireline logging [B,C]
survey

Run tubing and packer [C]

Install electric lines [F]

Set fencing [A]

Attach to field [A]
injection line

Set triplex pump [A]

Set 2 frac tanks [A,D]

Set filtration unit [A]

Set small pumps [A]

Install plumbing, [A]
valves, and meters

Install electric [A,E]
panel and outlets

Get molasses on location [D]

Connect molasses truck [A]
to injection system

Prepare injection [A]
mixture

Begin
Injection

Contracted Services

A) roustabout crew
B) logging company
C) pulling unit and crew
D) truck
E) electrician
F) electric company
G) dozer and landwork

Figure 2-2: Plan for Injection Well Facility Installation
(The plan reads from right to left.)

Procedure for Nutrient Treatment Injection

Molasses Arrives

Pump Molasses from Heated Truck to Frac Tank 1

Pump Brine into Frac Tank 1

Circulate 50/50 Brine/Molasses Mixture in Frac Tank 1 (Roll)

Add Ammonium Nitrate to Frac Tank 1

If Heated Truck has capacity, add brine to it and circulate to reduce the viscosity of the fluid
in the Heated Truck and increase Molasses recovery from the truck.

Pump 50/50 Mixture from Frac Tank 1 through Filter Unit to Frac Tank 2

(Replace Filter Elements as needed)

Circulate Frac Tank 2

Inject 50/50 mix in Frac Tank 2 into Main Injection Line
(for a resulting 10/90 molasses/brine mix in Main Line)

Alternative:

Add Brine to Frac Tank 2 to 10/90 molasses/brine mix

Inject 10/90 mix into well

Figure 2-3: Procedure for Nutrient Treatment Injection
(The plan reads from left to right.)

18

PRODUCTION WELL INSTALLATION

Build pads [G]

Improve location [G]
and roads
(if necessary)

Remove current wellhead [A]

Wireline logging [B,C]
survey

Pull tubing [C]

Set tubing anchor [C]

Set tubing [C]

Set pump (downhole) [C]

Set rod string [C,A]

Set wellhead (christmas tree) [A]
stuffing box, piping,
valves, sampling line,
meter

Install electric line [F]

Set fencing [A]

Connect to gathering [A]
system

Set pumping unit [A,D]

Set electric panel [E,A]

Set electric motor [E,A]

Begin
Pumping

Contracted Services

A) roustabout crew
B) logging company
C) pulling unit and crew
D) truck
E) electrician
F) electric company
G) dozer and landwork

Figure 2-4: Plan for Production Well Facility Installation
(The plan reads from right to left.)

19

1 Gunbarrel Separator
2 Water Tank
1 Oil Tank

Injection Pump

5-1

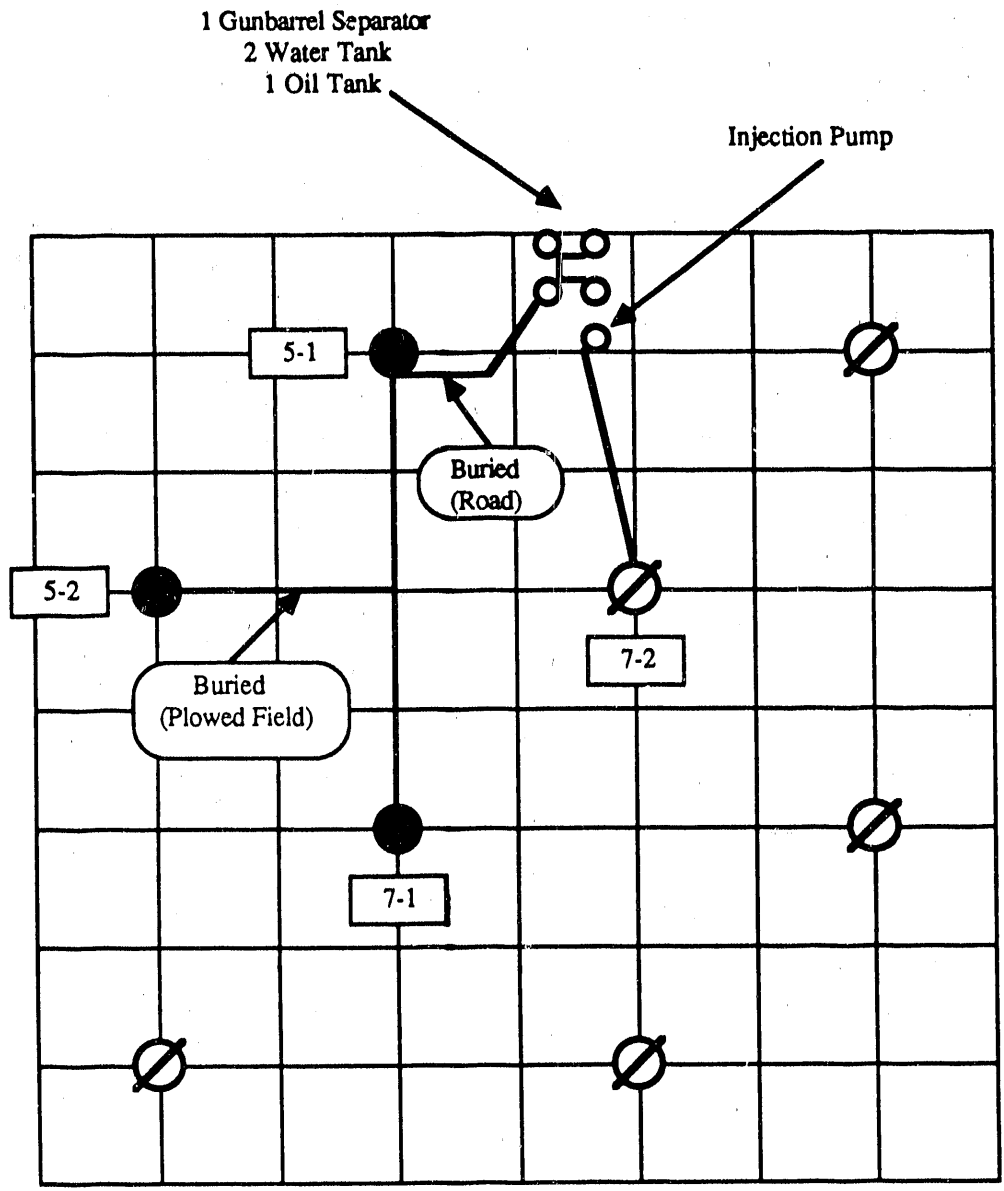Buried
(Road)

5-2

Buried
(Plowed Field)

7-2

7-1

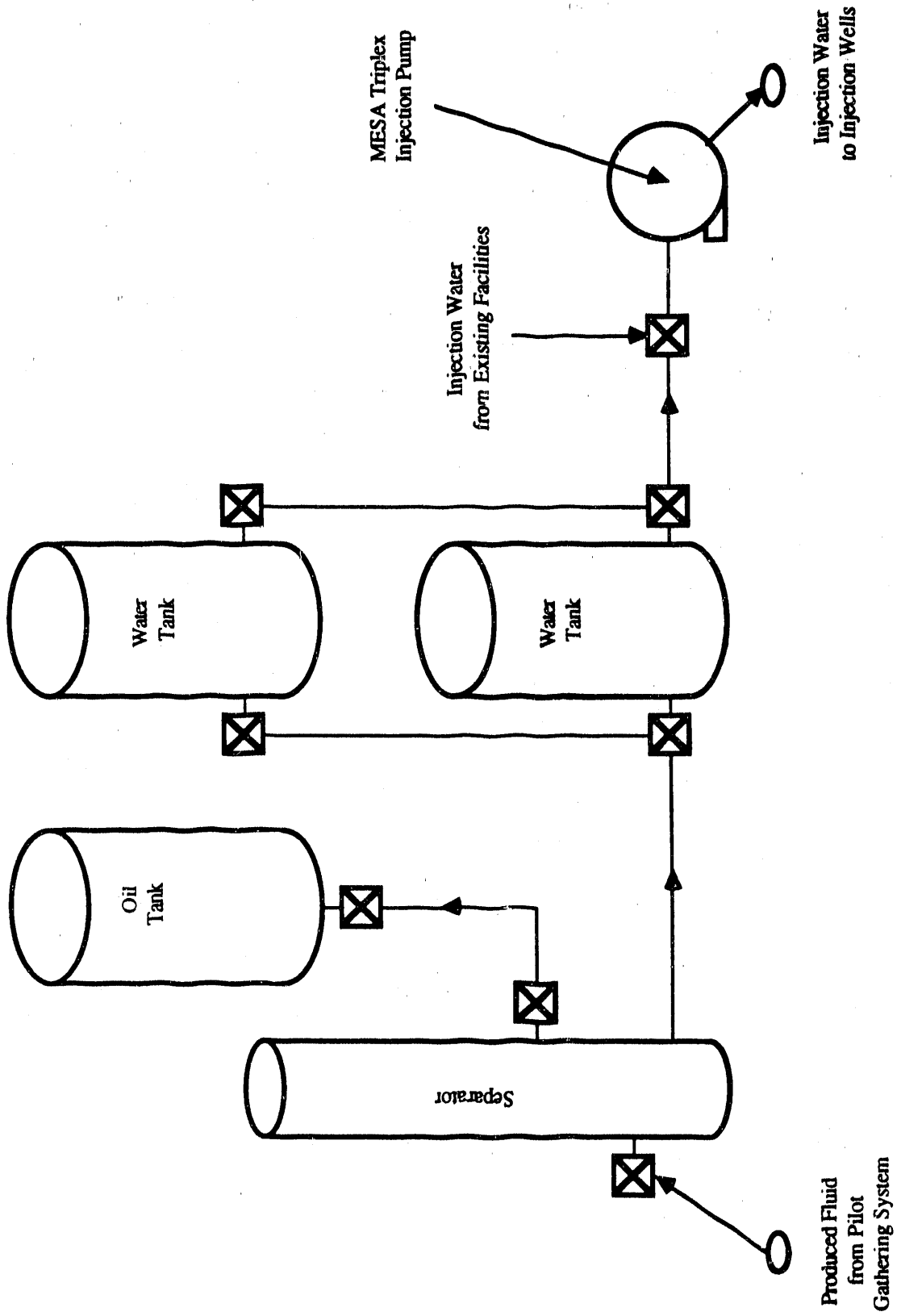Figure 2-5 Gathering System Design

Figure 2-6 Separator and Tank Batteries

3. The Southeast Vassar Vertz Sand Unit (SEVVSU)

The field chosen for this pilot study is the Southeast Vassar Vertz Sand Unit. Figure 3-1 is a map of the geological regions of the state of Oklahoma [Oklahoma Geological Survey, 1972]. As indicated in the figure the Southeast Vassar field is located about 50 miles north northeast of Oklahoma City, Oklahoma. It is located on the northern shelf area of the Anadarko Basin. The Vertz sandstone belongs to the Wabaunsee Group of Pennsylvanian age.

The Southeast Vassar field was discovered in 1966. It was unitized in 1974 and a line drive waterflood was initiated. The flood runs from southwest toward the northeast. As each production well exceeded a 10 to 1 water-oil ratio, it was converted to an injection well. The injection wells behind the active injectors are used to maintain pressure to insure that injected water continues to drive to the northeast. These pressure maintenance wells take little or no water. By 1987, the line of active injector wells was along the east edge of the southwest quarter of section 13.

The Vertz sandstone was probably formed by a meandering stream depositional system. Willhite [1986] presents an example of such an environment in his Figure 7.38. The Vertz is a uniform well-ordered sandstone which fines upward very gradually and has a basal lag of pebble size clasts. The sandstone has little vertical permeability variation and the preferential horizontal permeability lies in the paleocurrent direction. In a meandering stream system, a channel may become cut off forming an oxbow lake. If the abandoned channel is not subsequently reworked prior to system burial, it will fill with silt and form a clay plug. This will create a permeability barrier in the sandstone reservoir.

A net sand isopach of the Southeast Vassar Vertz Sand Unit is shown in Figure 3-2. Here, each major grid represents a quarter section. The solid line north of Well 5-1 and angling upward through the northwest quarter of section 13 is the location of a

22

permeability barrier in the field. The barrier has been identified by the dry hole in this area and the lack of communication of flood waters across the barrier. To the southeast, the zero thickness line is broken since the true extent of the reservoir in this region is not known. The flow path of the depositional stream system appears to have been from northeast to southwest. This is likely the direction of the preferential permeability in the reservoir.

The isopach map is the result of reinterpreting the geological model of the reservoir developed by Tenneco and a reservoir characterization simulation study performed at the University of Oklahoma [Knapp, et al., 1989a, and Knapp, et al., 1989b]. The earlier geologic interpretation contained very little thickness in the southeast quarter of section 13. The simulation study indicated that more reservoir volume was necessary to support the production from the two wells located in that quarter section. A step-out development well (8-3) was drilled near the center of the southeast quarter (see Figure 3-2). Under the old interpretation this well should have encountered 2 to 4 feet of pay. The new well had 14 feet of pay. Elements of the geologic interpretation of the reservoir done after the completion of this well (8-3) are incorporated into the isopach map.

A fine grid simulation study of the SEVVSU is underway. The latest geological interpretation indicates that the permeability barrier isolates the northwestern part of the field from the region to the southeast. Based on this assumption, the fine grid model (Figure 3-3) only models the southeast portion of the field. The isopach map also changes slightly in response to the latest model. The grid is a single layer, two-dimensional, areal model of the reservoir. The grid has its maximum density in the region of the field pilot. The simulator used in this study is the BOAST II simulator [Fanchi, et al., 1987].

By May 1989, the cumulative oil production from the Southeast Vassar was 2.4 million stock tank barrels (STB) and 14 wells were operating as injectors or producers.

The formation has a vertical depth of around 1800 ft. The original reservoir pressure was 850 psi. at 92oF. Hydrometer readings have given oil gravities from 38 to 42 degrees API. From gas chromatography, gas gravities of from 0.70 to 1.18 (air = 1.0) have been measured. In the reservoir simulation study, an oil gravity of 40 degrees API and a gas gravity of 0.85 were used. The oil and water viscosities are 2.9 cp and 1.1 cp, respectively.

The Dykstra-Parsons permeability variation factor [Dykstra and Parsons, 1950], was 0.35 from core permeabilities indicating little vertical variability in permeability. Consistent with this is the high recovery obtained by the waterflood. In the region of the reservoir behind the flood front, it is estimated that primary and secondary recovery methods have produced almost 60% of the original oil in place. The mobile oil phase in the region planned for the pilot study may be as low as 5% of the original oil in place.

The microbial field pilot study is planned for the southwest quarter of section 13 behind the line of active waterflood injectors. Pumping units will be installed on wells 5-1, 5-2, and 7-1. The 7-2 well will become the injector for the pilot after workover operations to restore injectivity. With the three producers establishing a drawdown to the west and the active injectors functioning to the east, it is expected that all water injected in well 7-2 will be confined to the pilot area. Production and injection data on the four pilot wells will be collected for at least one month prior to nutrient injection to establish a baseline of reservoir performance. One thousand barrel slugs of approximately 10% nutrient solution will be injected into the injection well weekly for three months. This will be followed by continuing the waterflood. The production rates and pressures will be monitored and fluids sampled at the production wells until the reservoir has stabilized or for 18 months.

Based upon the current interpretation of paleocurrent direction, the preferential flow path is believed to be from the 7-2 to the 7-1. The effects of the injection are expected to be first seen at the 7-1 well. If the microbial process works as expected, this

24

path will experience a permeability reduction caused by the **in situ** growth of microorganisms. Later volumes of injected water will be diverted to wells 5-1 and 5-2. The goal of the pilot is to demonstrate that the flow paths can be changed in this region due to the growth and metabolism of indigenous bacteria. The field pilot may enhance oil recovery by sweeping some of the previously bypassed oil.

Between the time the proposal was submitted to the Department of Energy and its subsequent funding, the Southeast Vassar Vertz Sand Unit working interest owned by Tenneco Exploration and Production Company (the unit operator) was sold to Mesa Limited Partnership. Conversations between the principal investigators, University Legal Counsel, and Mesa Limited Partnership have resulted in an agreement for the future operation of this field pilot study. This agreement was executed in late September 1989. Mesa has agreed to allow the continued use of the field and provide some technical assistance in the installation and operation of the field pilot.

References

Dykstra, H. and R.L. Parsons, 1950. "The prediction of oil recovery by waterflood", Secondary Recovery of Oil in the United States, API, pp. 160-174.

Fanchi, J.R., J.E. Kennedy, and D.L. Dauben, 1987, "BOAST II: A Three-Dimensional, Three-Phase Black Oil Applied Simulation Tool", DOE/BC-88/2/SP, National Technical Information Service, Springfield, VA.

Knapp, R.M., J.L. Chisholm, M.J. McInerney, D.E. Menzie, 1989a, "Pre-test Studies and Design for a Microbially Enhanced Oil Recovery Field Pilot Study", Proceedings of the Eighth Tertiary Oil Recovery Conference, March 8-9, 1989, Wichita, KS.

Knapp, R.M., M.J. McInerney, D.E. Menzie, R.A. Raiders, 1989b, "Microbial Field Pilot Study", Final Report, U.S. DOE/BC/14084-6, National Technical Information Service, Springfield, VA

Oklahoma Geological Survey, 1972, Geology and Earth Resources of Oklahoma, University of Oklahoma, Norman, OK.

Willhite, G.P., 1986, Waterflooding, SPE Textbook Series, Vol. 3, Society of Petroleum Engineers, Richardson, TX, p. 244.
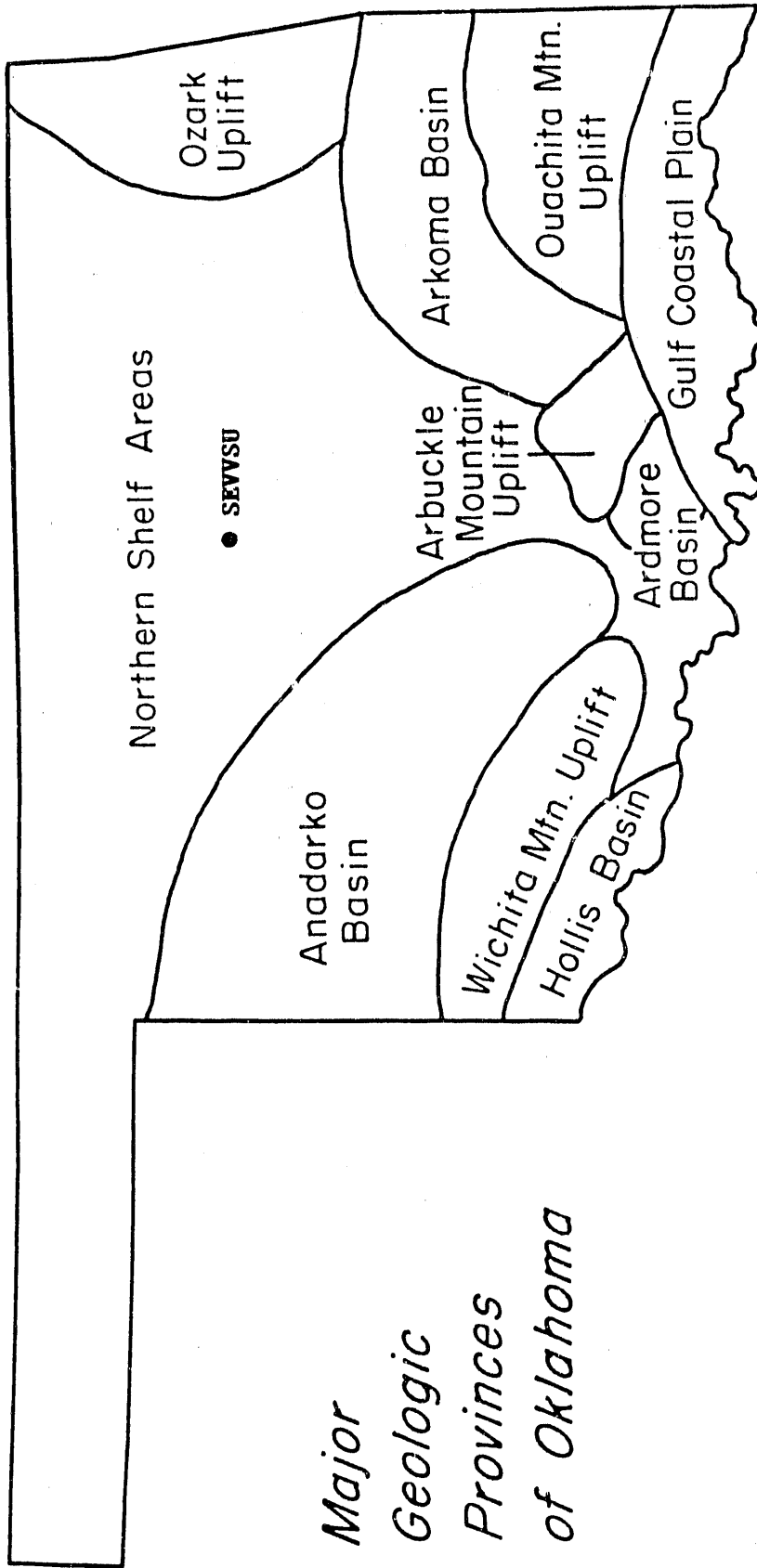
Major
Geologic
Provinces
of Oklahoma

Northern Shelf Areas

Ozark Uplift

Arkoma Basin

Ouachita Mtn. Uplift

Gulf Coastal Plain

• SEVVSU

Arbuckle Mountain Uplift

Ardmore Basin

Anadarko Basin

Wichita Mtn. Uplift

Hollis Basin

3-1. Oklahoma Geological Regions
(After Oklahoma Geological Survey, 1972)
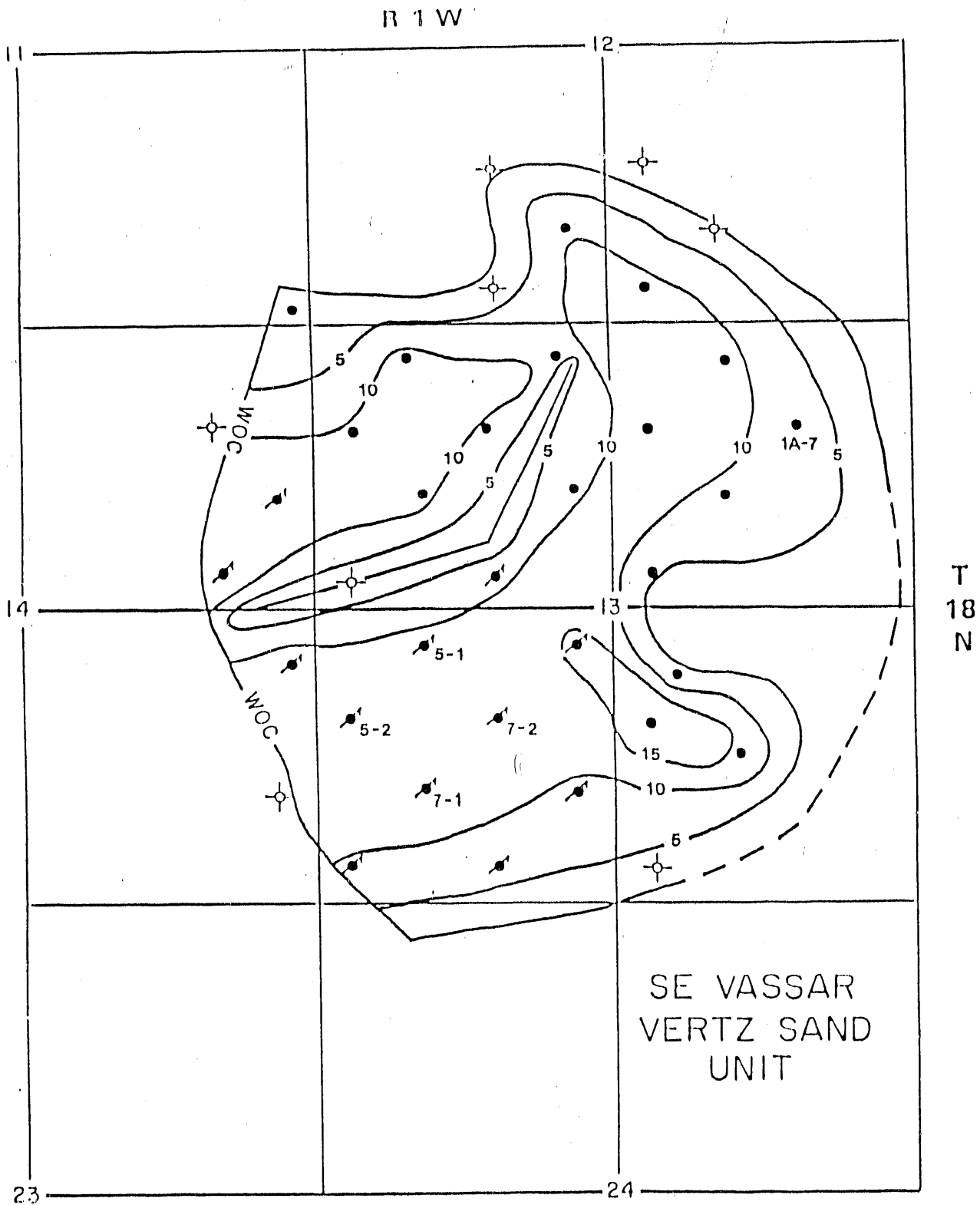
3-2. Net Thickness Map of Southeast Vassar Vertz Sand Unit (SEVVSU)
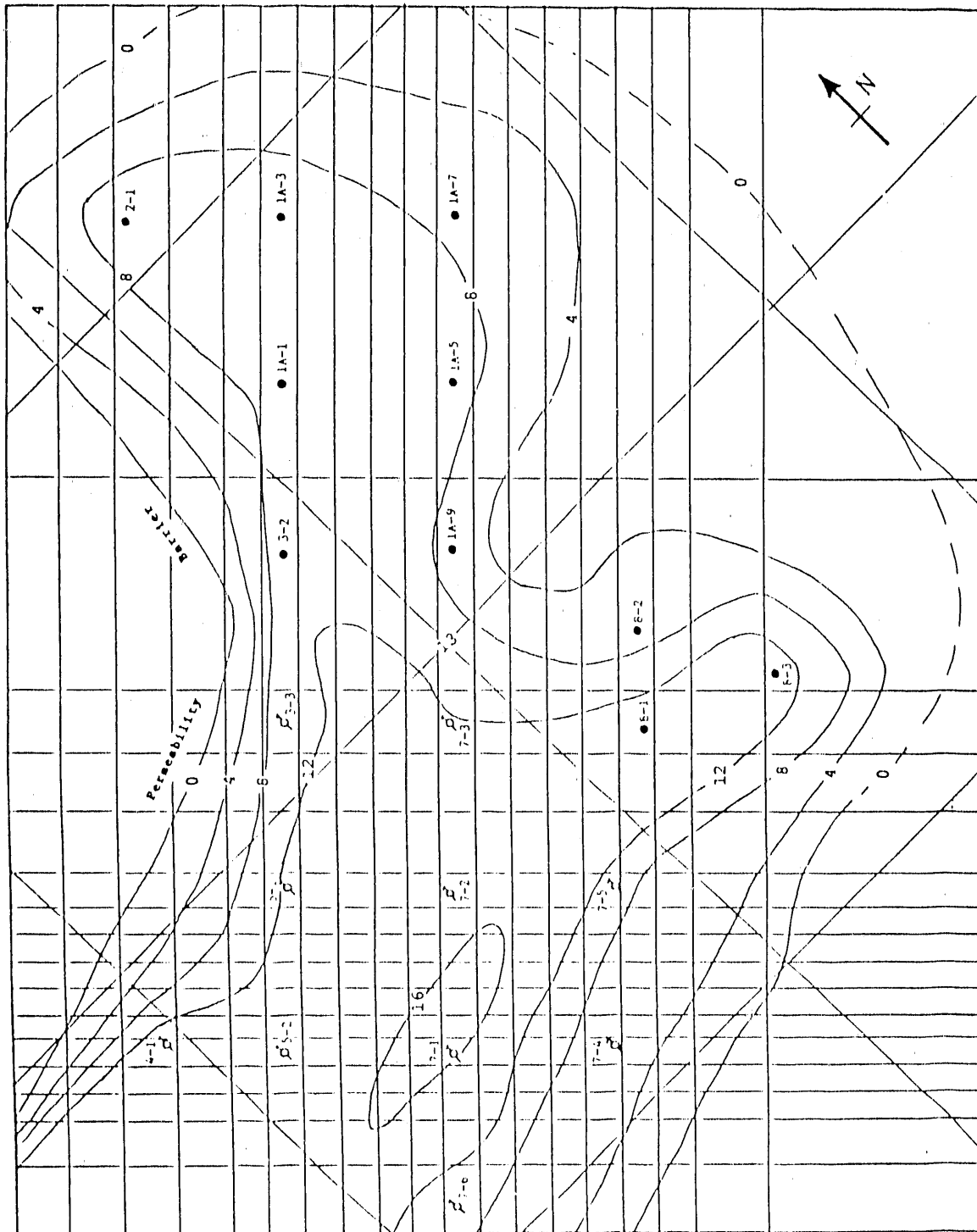
3-3. Grid Block Diagram For Fine Grid Simulation with Net Thickness Map of South SEVVSU

4. CORE FLOOD EXPERIMENTS

4.1 INTRODUCTION

Microbially enhanced oil recovery (MEOR) is an emerging technology that has the potential to recover a portion of the residual oil remaining in reservoirs after waterflooding. Some of the unique advantages of MEOR are the ability to preferentially plug high permeability zones by multiplication of cell mass and the production of metabolic products. However, to ensure a high rate of success in the field, the mechanisms by which microorganisms enhance oil recovery must be understood.

4.2 MECHANISMS OF MICROBIAL ENHANCED OIL RECOVERY

The literature shows that there are three major mechanisms by which microorganisms may be used to enhance oil recovery:

(a) by selective plugging of formation flowpaths;

(b) by changing the chemical and/or physical properties of the reservoir fluids

(c) by destruction or alteration of the rock formation

Selective plugging of formation flowpaths

Almost all producing zones have variable permeability due to stratification, depositional environment, or diagenesis. This phenomena creates preferential flow paths for the displacing fluid (water). The invading fluid moves rapidly through the more permeable zones and more slowly in the less permeable zones. Once a continuous flow path has been established between the injection well and the production well,

an increasing portion of injection water flows along this path. Thus, more oil is swept from the higher permeable zones, and less from the lower permeable portions. This reservoir heterogeneity greatly affects the recovery efficiency of the fluid displacement process. Selective plugging of these high permeability zones by microorganisms can improve sweep efficiency. Two types of microbial plugging have been identified: plugging by non-viable cells and plugging by viable microorganisms.

In early studies, non-viable microorganisms were used to study the plugging mechanism. Merkt [1943] was the one of the first to report the use of microorganisms in changing the permeability. Since dead cells do not produce slime, precipitates, etc, non-viable cells can only act as particlulate agents. Kalish, et al [1964] found that slime-forming and aggregated viable bacteria had a greater effect on permeability reduction per bacterium injected than did non-slime-forming or smaller bacteria (non-viable).

Since viable microorganisms can produce extracellular polymers, precipitates, etc. through their metabolic activity, the use of viable microorganisms should be able to recover more tertiary oil than the use of non-viable microorganisms. Viable microorganisms have the ability to adhere to the rock and produce an extracellular polysaccharide which covers the cells and the rock surface forming a polymer film. These actions result in more effective plugging than particulate plugging by dead cells. As the bacteria flourish and reproduce these activities exponentially increase. Thus, the cells become an effective plugging agent.

Crawford [1961,1962] was one of the first investigators to suggest the in-situ growth of bacteria could rectify permeability stratification. Since injection water tends to follow the least resistant flow paths, or highest permeability zones, bacteria transported with injection water will concentrate in those parts of the reservoir. With the

31

ability of microorganisms to multiply themselves in-situ, higher permeable zones would be blocked by this mass of cells, and divert subsequent flow to lower permeability zones.

Myers and Samiroden [1967], Jenneman, et al [1983,1984], Torbati, et al [1986], Raiders et al. [1985,1986a,1986b], Jack et al. [1982], and Bryant and Douglas [1987] have all investigated the effects of viable microorganisms in porous media. One or more have concluded that viable microorganisms can penetrate porous media, reduce permeability by as much as 90%, preferentially plug higher permeability zones and larger pores, and produce chemicals and gases which improve recovery.

Chemical changes and processes affecting reservoir fluids

Several chemical changes occur as a result of the MEOR processes which affect the fluids in the reservoir. Microbial processes result in a change in the relative permeability relationship from two phases to three phases. The metabolism of many microorganisms may result in the production of carbon dioxide, nitrogen, or possibly methane, which can create a free gas phase in the reservoir. A free gas phase has been found to decrease residual oil saturation. Holmgren and Morse [1951] used Nellie Bly sandstone to study waterflood recoveries with varying initial gas and oil saturations. They observed that increasing the initial free gas saturation caused the residual oil saturation to decrease. The presence of a gas phase caused a decrease in residual oil saturation of six to ten percent of pore volume. The generation of a free gas phase in a core without one can account for a fifth to a third of the residual oil recovered after waterflooding. Kyte et al. [9] conducted experiments on water-wet and oil-wet cores. They found that lower residual oil saturations were obtained at successive flooding stages when gas was present compared to those floods performed in the

absence of gas. Greater reductions in residual oil saturations occured in the presence of increasing mobile gas saturations of up to 15%. With further increases in initial gas saturations, the corresponding reductions in residual oil saturations become less pronounced.

Biosurfactants and cosurfactants (alcohols) are produced as a byproduct of the MEOR process (Javaheri, et al [1985]). Surfactants lower the interfacial tension at the oil-water interface and displace oil that cannot be displaced by water alone. Capillary forces that trap residual oil in porous media are reduced by lowering interfacial tension. One of the problems of surfactant flooding is the adsorption of surfactant on the surface in the reservoir rock. This decreases the concentration of the surfactant below that required to perform the task. This problem maybe less likely to occur if the surfactant could be produced in-situ.

Oil displacement by water from a porous system is believed to be governed by competition between viscous and capillary forces. Melrose and Bradner [1974] introduced the term capillary number (N_{ca}) to relate the magnitude of viscous forces to the magnitude of the capillary forces. They define it as:

$$N_{ca} = \frac{V\mu_w}{\sigma_{ow}}$$

(1)

where

N_{ca} : capillary number, dimensionless

V : interstitial velocity, $\frac{u}{\phi}$

μ_w : viscosity of displacing fluid

σ_{ow} : interfacial tension between oil and the displacing fluid

The reduction in interfacial tension caused by the in situ surfactant and

33

alcohol generation increases microscopic displacement efficency in the porous medium and reduces the residual oil saturation (Moore and Slobod [1956]). This is illustrated in Figure 4-1 by the capillary desaturation curve (after Stalkup [1984]) where the non-wetting phase (oil) residual saturation is plotted as a function of dimensionless capillary number. At low values of the capillary number ($< 10^{-6}$), the residual oil saturation is nearly constant. In this region the residual oil saturation is almost independent of viscous forces. At the critical value of N_{ca}, above which residual oil saturation decreases, the displacement process is in a transition from one dominated by capillary forces to one controlled by competition between viscous forces and capillary forces. Further increases in capillary number result in decreases in residual oil saturation and improved oil recovery.

The effective permeability reduction factor (PRF) can be defined as:

$$PRF = \frac{K_{wi}}{K_{wsor}} 100 \qquad (2)$$

where:

      PRF : effective permeability reduction factor, percent

      K_{wi} : effective brine permeability of the core during i-th treatment, mD

      K_{wsor} : effective brine permeability of the core at residual oil saturation, mD

In MEOR processes, a series of nutrient treatments are used to improve oil recovery. The incremental oil recovery associated with each nutrient treatment is the oil produced by the release of pressure caused by the in situ gas produced during incubation of the core with nutrients plus the oil that is produced by the injection of the subsequent treatment. The recovery factor (RF) is defined as:

$$RF = \frac{N_p}{OIPW}\ 100, \quad \% \tag{3}$$

where

N_p : cumulative oil production after MEOR treatments, ml

OIPW : Oil In Place after Waterflood ($S_{or}*PV$), ml

A relationship between the capillary number after i treatments, N_{ca}^i, and the capillary number before treatment, N_{ca}^o, can be developed. This relationship is based on the definition of capillary number and permeability reduction factor (PRF). If the viscosity of water and the Darcy velocity are unchanged by the treatment, then:

$$\left[\frac{N_{ca}^i}{N_{ca}^o}\right] = \left[\frac{\phi_o}{\phi_i}\right]\left[\frac{\sigma_{ow}^o}{\sigma_{ow}^i}\right] \tag{4}$$

A correlation of the rate of change in porosity versus the rate of change in permeability due to selective plugging by microorganisms was introduced by Civan et al. [1988]:

$$PRF = \frac{K_i}{K_o} = \left[\frac{\phi_i}{\phi_o}\right]^3 \tag{5}$$

Substituting this expression into the capillary number ratio expression results in:

$$\left[\frac{N_{ca}^i}{N_{ca}^o}\right] = \left[\frac{1}{PRF}\right]^{1/3}\left[\frac{\sigma_{ow}^o}{\sigma_{ow}^i}\right] \tag{6}$$

Formation destruction

Acids are produced by certain bacteria as a byproduct of metabolism. If the

porous medium is a carbonate (limestone) or has carbonate cement between individual clasts, then acid production can modify the rock system. It is not known whether in situ metabolic acids can be produced in sufficient quantities to have significant effects on the lithology of carbonates.

4.3 EXPERIMENTAL ANALYSIS

The experiments described in this section were conducted to provide information about the mechanisms of oil recovery caused by microbial activity within a core. Specifically, samples of microorganisms from one of the wells in the Southeast Vassar Vertz Sand Unit (SEVVSU), Payne County, Oklahoma were investigated for their potential in microbial enhancement of oil recovery. All experiments were performed using oil and brine taken from the SEVVSU. The NaCl salinity of the brine was around 15%. The experiments were performed at reservoir temperature.

Core preparation

Cores, two inches in diameter and six inches in length, were cut from Berea sandstone. Initial permeability values ranged from 84 to 724 md. The cores were cleaned by extraction with toluene and then were steam cleaned to remove humic acid and organic matter. After steam cleaning, the cores were dried at 125°C. The cores were prepared for flooding according to the method of Menzie [1988] with a pressure tap installed at the midpoint of the core.

Figure 4-2 shows a schematic of the experimental apparatus used. A positive displacement metering pump was used to inject liquids into the core. The core assembly was placed in an oven at constant temperature of 35°C. A 50 ml plastic syringe

with a Luer lock was used to collect the effluent from the downstream end of the core. The use of the syringe provided a simple method to collect all three phases distinctively by gravity segregation and avoided air contamination.

Each core was flushed with carbon dioxide to provide an anaerobic environment and then flooded with Vertz brine flushed with nitrogen to minimize oxygen content. The porosity was determined gravimetrically. The absolute permeability was measured (Jenneman, et al [1984]) and the core flooded with Vertz crude oil to irreducible water saturation. The core was then flooded with brine to irreducible (residual) oil saturation. The effective brine permeability of the core was determined. After these steps, each core was treated with one or more inoculations of bacteria indigeneous to the Vertz sand unit. The bacterial population was enriched by adding 1% (vol/vol) molasses and 0.3% (wt/vol) ammonium nitrate NH_4NO_3 to brine collected from well 1A-9. The nutrient ammended brine was incubated at 32°C until growth occured. As many as 10 treatments of a nutrient mixture (Vertz brine + 1% molasses + .3% NH_4NO_3) were performed on each core. Injection rates (flow volume per unit time) were kept constant and low to assure laminar flow.

During each treatment, brine flow rates and differential pressures across the core were measured to determine the effective brine permeability of the core. The effective permeability reduction factor (PRF) was then determined for each treatment.

The effluent brines were analyzed to calculate carbon and nitrogen balances and to determine the surface tension. The gases were analyzed using a gas chromatograph. Volatile fatty acids and alcohol concentrations in the brine were determined on a gas chromatograph equipped with a flame ionization detector and a fused silica column. Carbohydrate and nitrate concentration in the brine were determined colorimetrically. For one of the cores, C06, the surface tension and viscosities of the

37

brines were determined. The surface tension of the influent and effluent brine was determined using a DuNouy ring tensiometer. Viscosity of the influent and effluent brine was determined using a Cannon-Fenske viscometer.

Theoretical calculations

In predicting the gas products in the effluent samples of each treatment, a theoretical balance of nutrient consumption was developed. These calculations provided an estimate of the products that formed as a result of metabolization by microorganisms. Molasses consists of various mono and disaccharides of hexose sugars. In the theoretical calculations, the empirical formula of a hexose, i.e. glucose, was used to represent all the carbohydrate in molasses.

The theoretical calculation of the product concentrations of hexose and nitrate result from a stoichiometric balance of the reaction equations. Microorganisms metabolize hexose to acetate (CH_3COO^-) and carbonate (HCO_3^-) in the presence of the electron receptor, nitrate, which is reduced to nitrogen. Combining these reactions gives the theoretical reaction:

$$5C_6H_{12}O_6 + 8NO_3^- \longrightarrow 10CH_3COO^- + 10CO_2 + 4N_2 + 9H_2O + 2H^+$$

The nutrient mixture used contained 1% molasses. This molasses was feed grade molasses consisting of 48% to 58% carbohydrates (hexose). The remainder being vitamins, minerals, other chemicals, and water. Assuming molasses is composed of 58% hexose sugers (glucose equivalents) leads to the following theoretical product concentrations in the effluent:

$$CH_3COO^- = 0.033 \ \frac{10}{5} = 0.067 \ \text{moles acetate/l}$$

$$CO_2 = 0.033 \; \frac{10}{5} = 0.067 \text{ moles } CO_2/l$$

$$H_2O = 0.033 \; \frac{9}{5} = 0.060 \text{ moles } H_2O/l$$

$$N_2 = 0.0376 \; \frac{4}{8} = 0.0188 \text{ moles } N_2/l$$

4.4 CORE EXPERIMENTS

Core experiments were performed on four Berea sandstone cores designated C06, C09, C10, and C11. For each nutrient treatment these cores were monitored for cumulative gas production (G_p), permeability reduction factor (PRF), and oil recovery factor (RF). The results are given for these experiments in Tables 4-1 through 4-4.

Core Number 06

During the waterflood, 2.6 PV of brine displaced 59.1% of original oil in place (OOIP) from core C06. Figure 4-3 shows permeability reduction factor (PRF), cumulative incremental oil recovery factor, and gas production for core C06. At the end of the treatments, approximately 10 PV of nutrient mixture had been injected and 84.2% of the oil in place after waterflooding had been recovered. This represents an additional 34.4% of OOIP. The total gas produced was 217.6 ml (at approximately 70°F and 1 atm.) with an average concentration of 70.2% of N_2 and 25.1% CO_2. At the end of the nutrient treatments, 2.6 PV of Vassar brine were injected through the core, and the PRF value stabilized at 4.9%.

In core C06, no significant oil and gas were recovered during the first three treatments. After three treatments, the microorganisms had acclimated to the environment and started to utilize the carbon sources, resulting in the production of biogenic gas and other microbial products. The surface tension of the effluent samples was found to be 52% of the injected nutrient mixture. The viscosity of the effluent was the same as the injected nutrient mixture.

Theoretically 232.6 ml of N_2 and 828 ml of CO_2 should have been produced by C06. Analysis of recovered gas indicates 147.8 ml of N_2 (63.5% of theoretical) and 67.4 ml of CO_2 (8.14% of theoretical) was produced.

Core Number 09

During the waterflood by 2.8 PV of Vassar brine, 58.1% of OOIP was recovered in core C09. Figure 4-4 shows PRF, cumulative incremental oil recovery and gas production for this core. At the end of eight treatments, after approximately 6 PV of nutrient mixture had been injected, an additional 22.6% OOIP was recovered for a 53.9% incremental oil recovery. The cumulative gas production was 135 ml with an average concentration of 65% N_2 and 6% CO_2. After the final nutrient treatments, 2.2 PV of Vassar brine were injected through this core and the PRF was stabilized at 15.5%.

Core Number 10

Core 10 developed extensive plugging on the injection face and produced very little oil and gas. Although six treatments were performed the permeability

reduction primarily occurred in the front half of the core. Figure 4-5 shows PRF, cumulative incremental oil recovery and gas production for this core. After injecting 1.9 PV of Vassar brine through the core at the final treatment, the FRF for the front half and back half of the core stabilized at 10.6% and 64% respectively.

Core Number 11

Core C11 was treated in a manner similar to the other cores. During waterflood, 2.3 PV of brine recovered 40.3% OIIP. Figure 4-6 shows PRF, cumulative incremental oil recovery and gas production. At the end of the sixth treatment, after approximately 5 PV of nutrient mixture were injected, 8.7% of incremental oil recovery or an additional of 5.4% OOIP was recovered. The total gas produced was 5.2 ml with an average concentration of 64% N_2 and 26% CO_2. After injecting 1.9 PV of Vassar brine through the core after the final treatment, the FRF stabilized at 15.7%.

Although experiment C11 recovered residual oil, recovery was much lower than cores C06 and C09. Despite attaining a low PRF, oil and gas production were not substantial. The core's initial permeability might explain low recovery since the original absolute permeability of the core was less than 100 md. The small amount of biogenic gas produced can also explain this low recovery. This result substantiates previous work done by Raiders et al. [1985] and Jenneman et al. [1983] indicating that low permeability appears to limit the microorganisms ability to proliferate and produce by-products.

4.5 DISCUSSION OF RESULTS

For Cores C06 and C09, as the permeability reduction factor started to decrease below 25%, oil recovery increased substantially. This suggests that microorganisms had preferentially plugged the higher permeability regions within the core and diverted the flow of the brine to the lower permeability (unswept) regions where more oil was trapped, apparently increasing the sweep efficiency of the flood. In C06, carbon and nitrogen analyses were also performed. CO_2, N_2, acetate, butyrate and ethanol were detected in the effluent samples. The results show that microorganisms proliferated and produced metabolic products that helped recover more oil.

Carbon recovery in the analyses was low. It was possible that other carbon components such as lactate were present in the effluent but were not detected by the gas chromatographic method used. The comparison of the theoretical calculations and experimental results for CO_2 shows that CO_2 recovery in the effluent was much lower than expected. This can be partially explained by the solubility of CO_2 in brine (in the form of H_2CO_3 or HCO_3^-) and in the oil. Further, since the Vertz brine has high concentrations of Ca^{++}, the carbon dioxide may have formed $CaCO_3$ which precipitated within the core. Finally, the amount of carbon involved in the production of cells is not accounted for in the empirical equation. The higher percentage of N_2 recovered and the complete consumption of nitrate in the later treatments suggests that the denitrification occured in the core.

The presence of biogenic gas in the core can explain some of the additional oil recovery. In most porous media the system is water wet, that is, the surface of the rock is in contact with water, the wetting phase. If present, oil and gas occupy the center of the pores with a buffer of water between them and the rock, and are con-

42

sidered non-wetting. The absolute permeability of the rock is the capacity of the rock to conduct fluid with only one phase present. Relative permeability is the fraction of this capacity available to a specific phase when multiple phases are present. Relative permeability is a function of the phase and the saturations of the phases present. Figure 4-7 depicts idealized wetting phase relative permeability, k_{rw}, and non-wetting relative permeability, k_{mw}, versus wetting phase saturation. In a core at residual oil saturation, the emergence of a free gas phase will increase the non-wetting saturation and oil will become more mobile. Based on the work of Holmgren and Morse [1951] this could account for the recovery of about a fifth to a third of the oil left after waterflooding.

Microscopic displacement efficiency also increased by changes in the chemical composition of the fluid. One of the products, ethanol is soluble in the oil. Ethanol production can increase microscopic displacement efficiency by decreasing the viscosity of oil. The surface tensions of the effluent brine samples were lower than the initial nutrient samples. This suggests that biosurfactant was also produced. Thus, microbial processes lead to reduction of the oil viscosity and surface tension which increase oil mobility and capillary number.

The growth of microorganisms within the core generates cellular material which reduces the porosity of the core. As microbial cells are produced, they attach to the walls of the pores. This reduces the volume of the pore which is available for fluid flow. Since all of the experiments were conducted at a constant volumetric injection rate, the fluid velocity in pores with microbial growth must have increased. Further, if some of the pore throats are completely blocked, the flow normally associated with these pores is diverted to other pores. Both of the above factors will lead to an increase in interstitial fluid velocity within those pores still available to fluid flow.

This increase in interstitial fluid velocity increases capillary number and oil recovery.

For core C06, using a stabilized PRF of 5% and a surface tension 52% of original value and assuming that the reduction in the interfacial tension between oil and water was the same as the reduction in surface tension, the change in the capillary number ratio for core C06 is

$$\left[\frac{N_{ca}^{i}}{N_{ca}^{o}}\right] = \left[\frac{1}{0.05}\right]^{1/3}\left[\frac{1}{0.52}\right] = 5.2$$

The capillary number after treatment was 5.2 times capillary number before treatment. From Figure 4-1, assuming $N_{ca}^{o} = 10^{-6}$, the increase of 5.2 in capillary number could have caused a decrease in residual oil saturation of 5% and the increase in capillary number could explain a 15 to 20% additional oil recovery.

4.6 CONCLUSIONS

(1) Increases in oil recovery were accompanied by production of biogenic gas, acids, ethanol and biomass by native bacteria collected from well 1A-9 of SEVVSU.

(2) Production of biogenic gas decreases the residual oil saturation due to relative permeability changes associated with the creation of a free gas phase in the reservoir. This can explain the recovery of a fifth to a third of the oil left after waterflooding.

(3) The increase in capillary number for core C06 can explain 15-20% additional oil recovery.

(4)   The mechanisms in conclusions (2) and (3) were active in the core experiments but do not fully explain the the additional oil production observed in cores C06 and C09. The contributions to recovery of other mechanisms, such as selective plugging, have not yet been quantified. Additional mechanisms which may be active have not yet been identified.

REFERENCES

Bryant, R.S. and J. Douglas. 1987. Evaluation of Microbial Systems in Porous Media for Enhanced Oil Recovery, presented at the Society of Petroleum Engineers International Symposium on Oilfield Chemistry, San Antonio, Tx, Feb. 1987.

Civan, F., R.M. Knapp, and H.A. Ohen. 1988. Automatic Estimation of Model Parameters for Swelling and Migration of Fine Particles in Porous Media, Paper presented at the AICHE Meeting in New Orleans, LA, (March 6-10, 1988).

Crawford, P.B. 1961. Possible Bacterial Correction of Stratification Problems, *Prod. Monthly,* vol 25, 10-11.

Crawford, P.B. 1962. Water Technology: Continual Changes Observed in Bacterial Stratification Rectification, *Prod. Monthly,* vol 26, 12.

Holmgren, C.R. and R.A. Morse. 1951. Effect of Free Gas Saturation on Oil Recovery by Waterflooding, *Transactions,* AIME, 192, 285-296.

Jack, T.R., B.G. Thompson, and E. DiBlasio. 1982. The Potential for Use of Microbes in the Production of Heavy Oil, Proceedings of the 1982 International Conference On the Microbial Enhancement of Oil Recovery, Afton, Oklahoma, (May 1982), 88-93.

Javaheri, M., G.E. Jenneman, M.J. McInerney, R.M. Knapp. 1985. Anerobic Production of a Biosurfactant by *Bacillus licheniformus* JF-2, Applied Environmental Microbiology, (September 1985), 689-700.

Jenneman, G.E., R.M. Knapp, D.E. Menzie, D.E. Revus, J.B. Clark, and D.M. Munnecke. 1983. Transport Phenomena and Plugging in Berea Sandstone Cores Using Microorganisms, In, E.C. Donaldson and J.B. Clark, (eds.) Proceedings of the 1982 International Symposium on Microbial Enhancement of Oil Recovery, Nat. Tech. Inf. Serv., Springfield, VA, CONF-8205140 71-75.

Jenneman, G.E., R.M. Knapp, M.J. McInerney, D.E. Menzie, and D.E. Revus. 1984. Experimental Studies of In-Situ Microbial Enhanced Oil Recovery, *Soc. Pet. Engr. J.,* (Feb. 1984) 33-37.

Kalish, P.J., J.E. Stewart, W.F. Rogers, and E.O. Benneth. 1964. The Effect of Bacteria on Sandstone Permeability, *J. Pet. Tech.,* vol 16, 805-814.

Kyte, J.R., R.J. Stanclift, Jr., S.C. Stephen, Jr., and L.A. Rapoport. 1956. Mechanism of Water Flooding in The Presence of Free Gas, *Trans.,* AIME 207, 215-221.

Melrose, J.C. and C.F. Brandner. 1974. Role of Capillary Forces in Determining Microscopic Displacement Efficiency for Oil Recovery by Waterflooding, *J. Cdn. Pet. Tech.,* (Oct. - Dec. 1974) 54-62.

Menzie, D.E., S. Dutta, and R.S. Shadizadeh. 1988. A New Method of Coating Oilfield Core for Laboratory Studies, *J. Pet. Tech.,* (May 1988) 643.

Merkt, E.E. 1943. The Effect of Bacteria on the Permeability of Oil Reservoir Rocks, Thesis, University of Texas, Austin, Texas, 14-29.

Moore, T.F. and R.L. Slobod. 1956. The Effect of Viscosity and Capillarity on The Displacement of Oil by Water, *Prod. Monthly*, (Aug. 1956) 20-30.

Myers, G.E., and W.D. Samiroden. 1967. Bacterial Penetration in Petroliferous Rocks, *Prod. Monthly*, (April 1967) 22-25.

Raiders, R.A., D.C. Freeman, G.E. Jenneman, R.M. Knapp, M.J. McInerney, and D.E. Menzie. 1985. The Use of Microorganisms to Increase the Recovery of Oil Form Cores, Paper SPE 14336 presented at the 60th Annual Meeting of the Society of Petroleum Engineers of AIME, Las Vegas, NV, Sept. 1985.

Raiders, R.A., M.J. McInerney, D.E. Revus, H.M. Torbati, R.M. Knapp, and G.E. Jenneman. 1986a. Selectivity and Depth of Microbial Plugging in Berea Sandstone Cores, *J. Indust. Microbial.*, (1986) 195-203.

Raiders, R.A., T.F. Maher, R.M. Knapp, and M.J. McInerney. 1986b. Selective Plugging and Oil Displacement in Crossflow Core Systems by Microorganisms, paper SPE 15600 presented at the 61st Annual Meeting of the Society of Petroleum Enginers of AIME, New Orleans, LA, Oct. 1986.

Stalkup, F.I., Jr. 1984. Miscible Displacement, Monograph series, SPE, Richardson, TX.

Torbati, H.M., R.A. Raiders, E.C. Donaldson, M.J. McInerney, G.E. Jenneman, and R.M. Knapp. 1986. Effect of Microbial Growth and Pore Entrance Size Distribution in Sandstone Cores, *J. Indust. Microbial.*, (1986) 227-234.

Table 4.1. Values of permeability reduction factor (PRF), recovery factor (RF), and cumulative gas production (G_p) for each treatment for Core C06.

Treatment	PRF %	RF %	G_p ml
0	100.0	0.0	0.0
1	74.6	5.0	0.0
2	60.0	7.4	1.0
3	71.5	17.3	8.0
4	67.6	24.8	9.1
5	26.2	34.7	17.1
6	21.8	45.1	38.6
7	15.5	52.5	15.5
8	20.0	62.4	88.6
9	18.0	68.3	119.1
10	11.0	73.7	148.1
11	15.3	78.2	173.1
12	13.3	82.2	194.1
13	8.0	84.2	198.6
14	4.9	84.2	217.6

Table 4.2. Values of permeability reduction factor (PRF), recovery factor (RF), and cumulative gas production (G_p) for each treatment for Core C09.

Treatment	PRF %	RF %	G_p ml
0	100.0	0.0	0.0
1	56.5	3.3	1.0
2	71.7	6.7	8.0
3	28.7	23.3	22.0
4	26.4	40.0	53.0
5	23.0	45.6	80.0
6	19.8	50.0	88.0
7	17.7	52.2	111.0
8	15.5	53.9	135.0

Table 4.3. Values of permeability reduction factor (PRF), recovery factor (RF), and cumulative gas production (Gp) for each treatment for Core C10.

Treatment	PRF %	RF %	G_p ml
0	100.0	0.0	0.0
1	49.0	0.1	0.1
2	30.9	0.1	0.1
3	13.8	0.1	0.1
4	12.8	0.1	0.1
5	10.6	0.1	0.3
6	10.6	0.1	0.3

Table 4.4. Values of permeability reduction factor (PRF), recovery factor (RF), and cumulative gas production (Gp) for each treatment for Core C11.

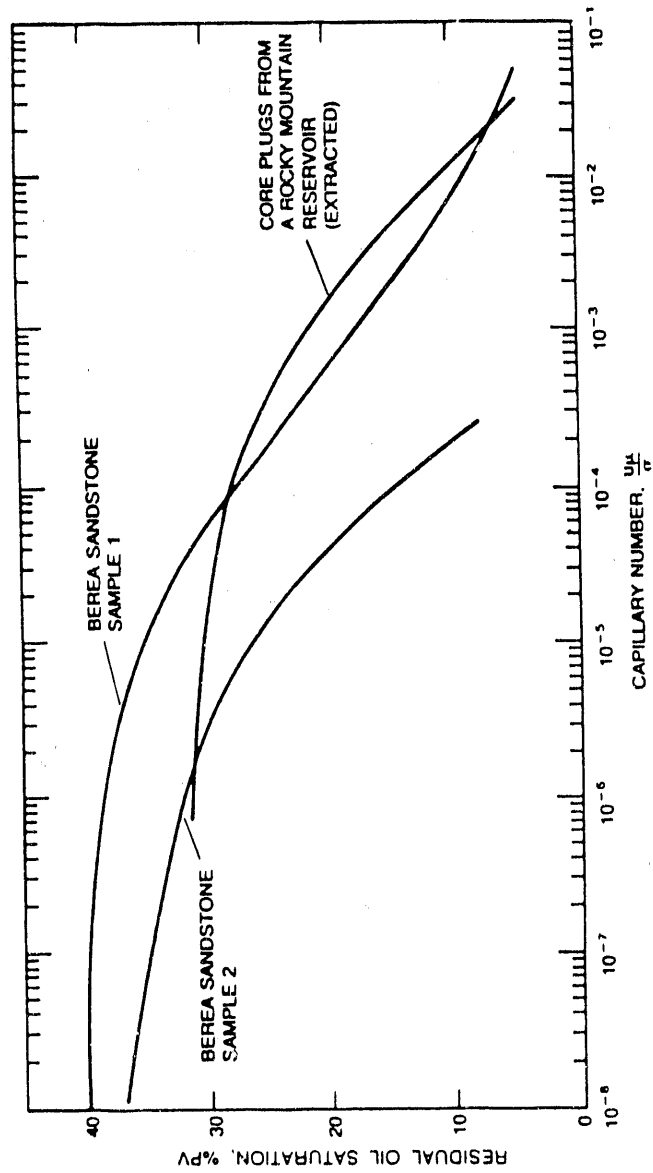| Treatment	PRF %	RF %	G_p ml
0	100.0	0.0	0.0
1	78.0	0.0	1.0
2	50.0	3.7	8.0
3	24.3	3.7	22.0
4	21.4	5.0	53.0
5	20.0	6.8	80.0
6	17.1	7.7	88.0
7	15.7	8.7	111.0
8	20.6	22.4	135.0

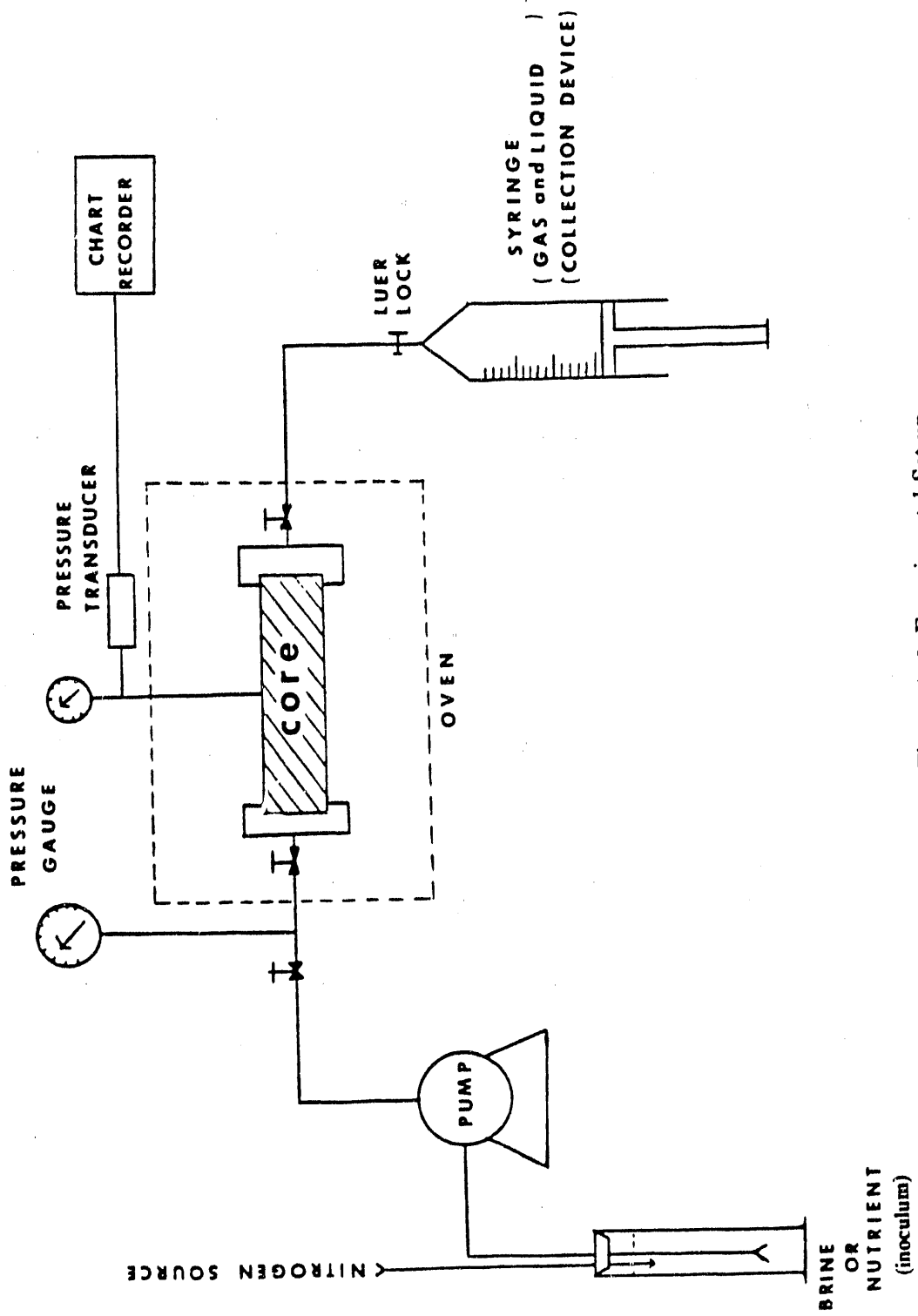Figure 4-1 Capillary Desaturation Curve (CDC)
(after Stalkup)

Figure 4-2 Experimental Set-up

Figure 4-3. Effect of nutrient treatments on the permeability
reduction factor (PRF), recovery factor (RF),
and gas production (Gp).

Core C09

Kabs = 219 md

Kw = 53 md

Porosity = 19.2 %

Sor(af. H20flood) = 30.4 % PV

Gp

RF

PRF

Number of Treatments

Figure 4-4. Effect of nutrient treatments on the permeability
reduction factor (PRF), recovery factor (RF),
and gas production (Gp).

Core C10

Kabs   = 152 md

Kw   = 9.4 md

Porosity   = 19 %

Sor(af. H20flood) = 36.8 % PV

——— GP
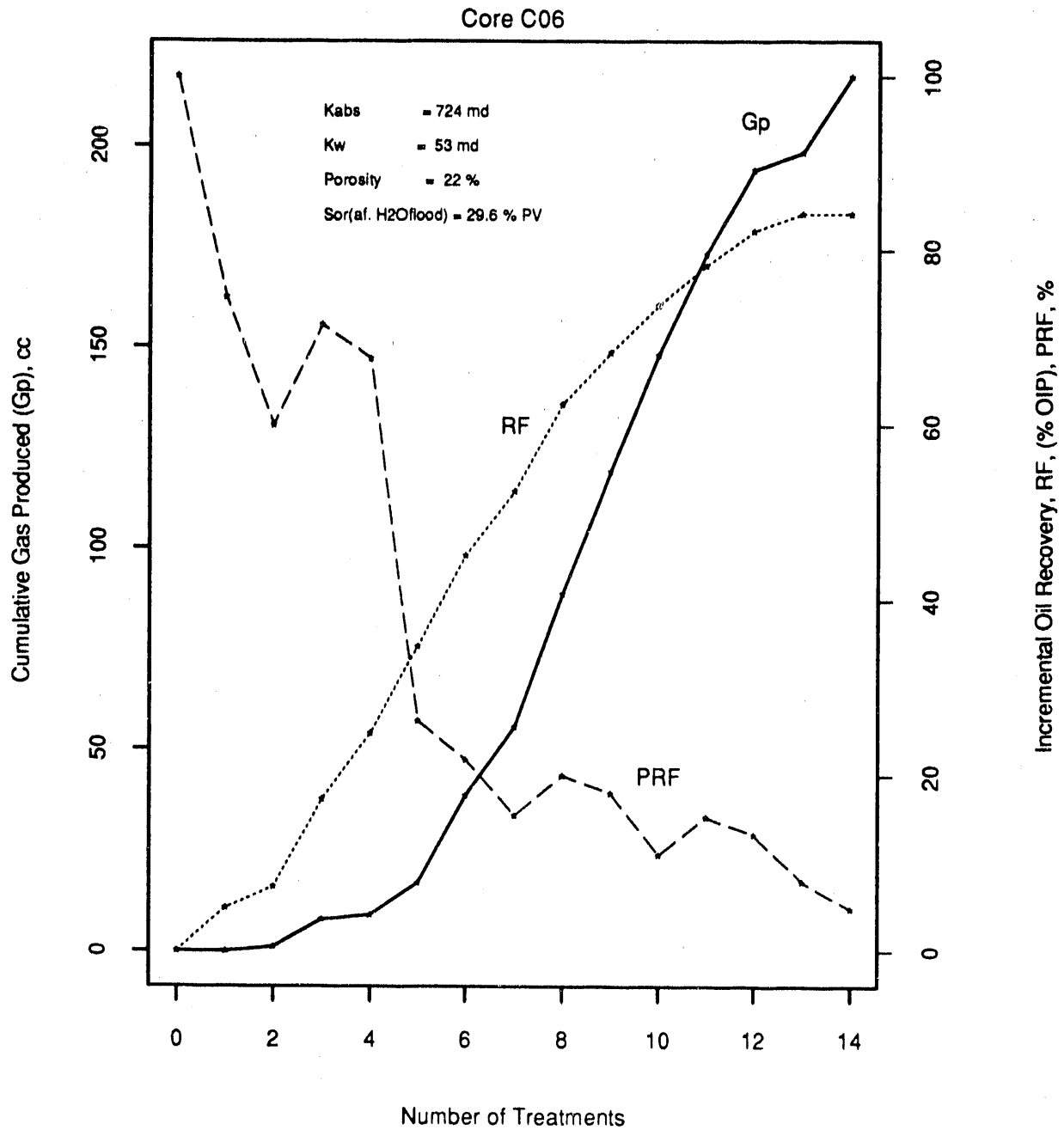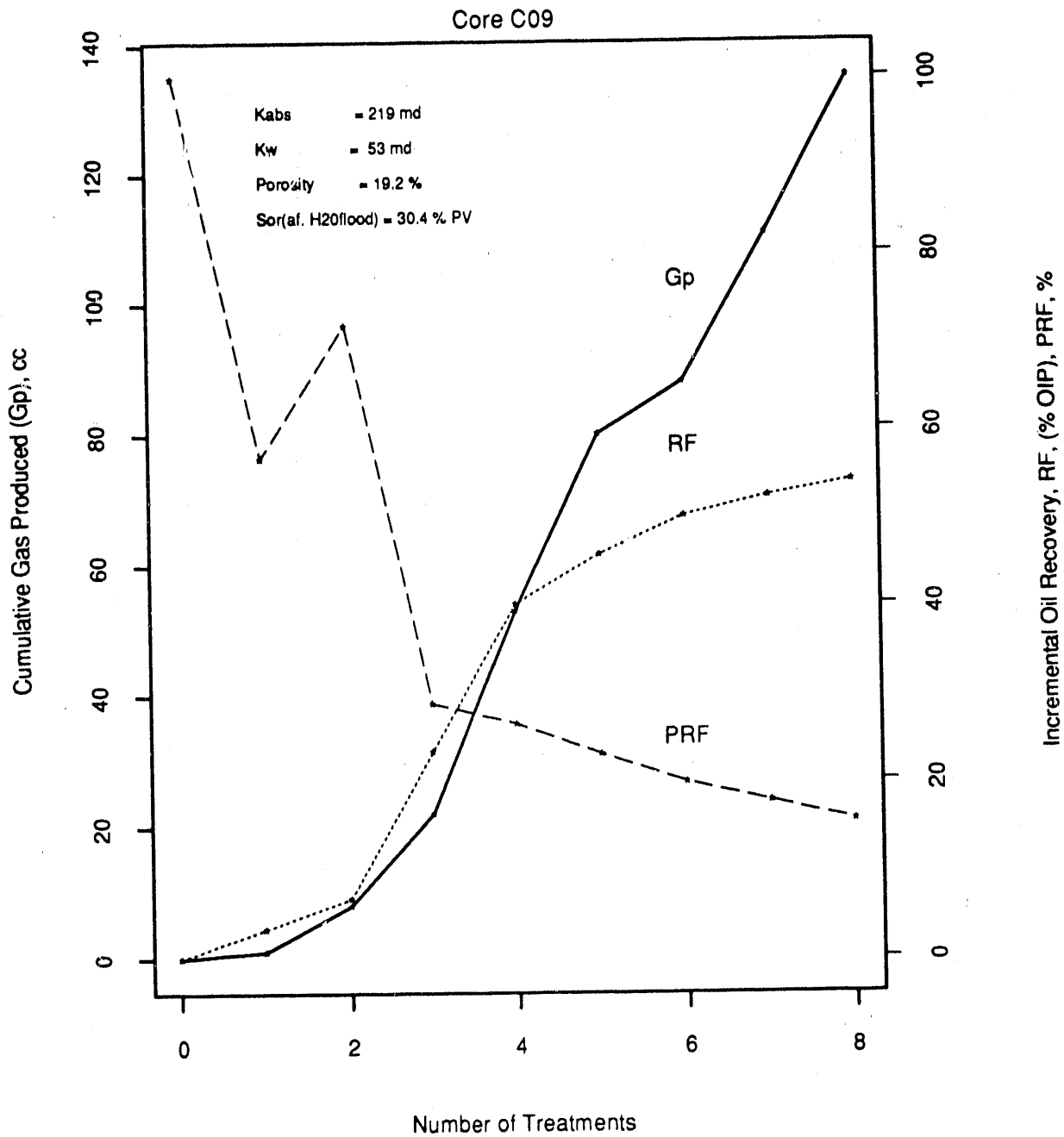
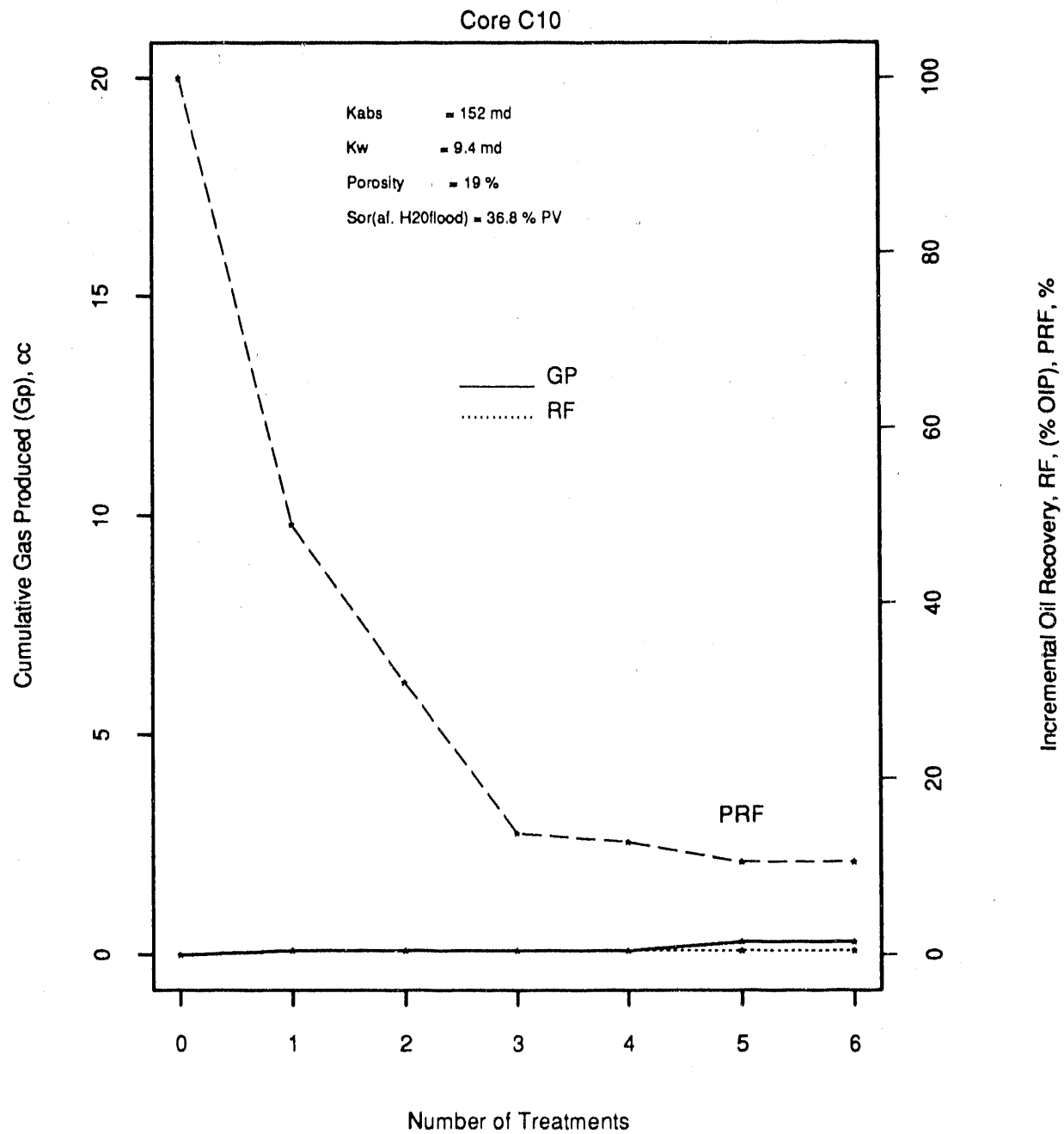············ RF

PRF

Number of Treatments

Figure 4-5. Effect of nutrient treatments on the permeability
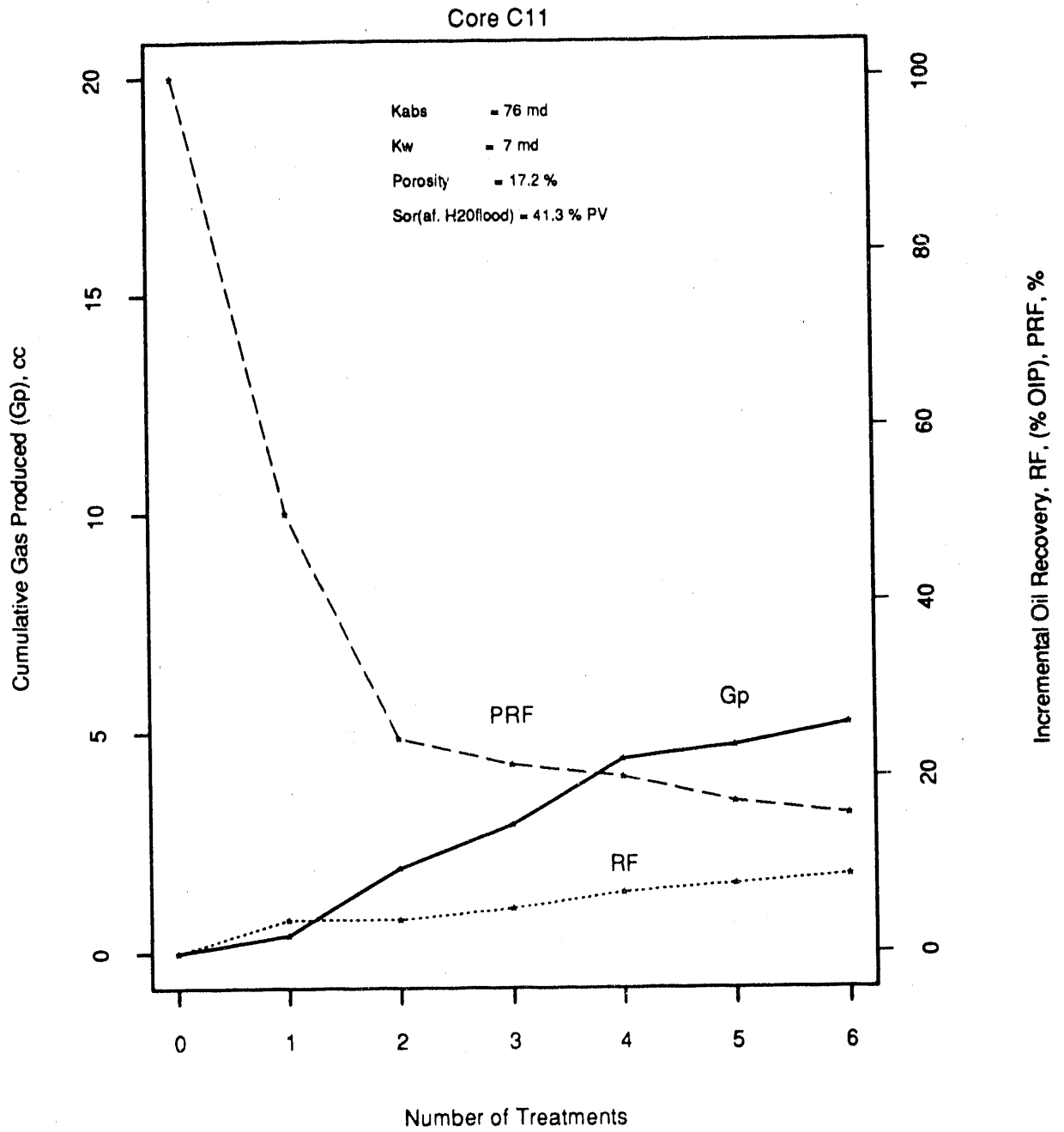reduction factor (PRF), recovery factor (RF),
and gas production (Gp).

54

Figure 4-6. Effect of nutrient treatments on the permeability
reduction factor (PRF), recovery factor (RF),
and gas production (Gp).

5. Bacterial Movement And Activity In Porous Subsurface Formations

5.1 Introduction

A detailed understanding of the mechanisms by which microorganisms penetrate subsurface formations is critical to the efficient and economical development of in situ microbially enhanced oil recovery technologies. Movement of bacteria through subsurface formations follows the movement of nutrients from septic tanks and leaking sewage pipes (Corapcioglu and Haridas, 1984). The enteric bacteria and viruses have been used to trace the movement of contaminated groundwater in much the same manner as chemical tracers are used (Keswick et al., 1982). Most of these studies are empirical in nature and have not addressed fundamental questions concerning the mechanisms of microbial movement. Such analyses are needed to evaluate and/or develop mathematical models which are required for the implementation of reservoir-wide processes.

In previous work, the biological factors important for transport of microorganisms through nutrient-saturated porous material under static conditions was studied (Reynolds et al., 1989). The penetration rates of a motile, non-chemotactic strain increased in a curvelinear fashion with the square of the core length, suggesting an ordered or band-like movement of cells through the core. According to this hypothesis, under conditions in which growth is restricted such as that in sand-packed cores, motile bacteria would consume practically all the locally available substrate, thereby creating a substrate gradient. Concomitantly, fermentation end products would accumulate and act as repellents. Both these conditions would stimulate the directional movement of the cells through the core. This mode of cell penetration and substrate utilization would resemble that found in plug-flow reactors (Pfeffer, 1980).

In this study, the mode of transport of a motile strain of *Escherichia coli* RW262 through anaerobic, nutrient-saturated, static, unconsolidated porous media was investigated. The data show that motile cells move through the core in a band-like fashion. Further, substrate use and metabolite production by bacterial cells in sand-packed cores was determined.

5.2 Materials and Methods

Bacterial strain and growth conditions : The motile, wild type strain of *Escherichia coli* RW262 (F^+ *mel-1 tan A sup F58* λ^-) was kindly provided by F. Ziamain, Max Planck Institute for Molecular Biology, FRG. The strain was grown anaerobically in galactose-nitrate mineral medium (GNM) containing (per 100 mL) : 0.45 g of galactose, 0.3 g of $NaNO_3$, 1.12 g of K_2HPO_4, 0.48 g of KH_2PO_4, 2 mL of Tanner's mineral solution (Table 1.2), and 1 mL of Tanner's trace metal solution (Table 1.3). The pH of the medium was 7.0. The strain was maintained on slants of GNM with 2% (wt/vol) agar and transferred every 15 days. After growth, the slants were stored at 4^oC. The motility of the strain was checked by inoculating MIO broth (Difco Laboratories).

Anaerobic media and solutions were prepared and used as described previously (Balch and Wolfe, 1976). The gas phase of all anaerobically prepared media and solutions was that of the anaerobic chamber, about 1 to 5% H_2 with the balance being N_2. The cell densities in anaerobically incubated sand-packed cores and broths at 23^oC were determined by viable cell count method. The counts were performed by serially diluting the sample in 20 mM phosphate buffer (pH 7.0) and inoculating duplicate plates of Plate Count Agar (Difco Laboratories). Colonies were counted after aerobic incubation of plates for 24h at 35^oC. The rate of growth of liquid cultures was also determined as the change in absorbance at 600 nm and the specific growth rate was calculated as described previously (McInerney et al., 1979).

Core experiments : Acid cleaned, commercially-available sand (100-to 200- mesh size) saturated in GNM was used to prepare the anaerobic, sterile porous medium. cm) and plastic cores (1.25 by 10 cm) were previously (Reynolds et al., 1989). The cores were d in a horizontal position inside the anaerobic chamber and inoculated with 0.2 ml of mid-exponential phase culture. Duplicate cores were used for each treatment. The penetration rate of cells (r_p), permeability (k), and pore volume of

each core were determined as described previously (Jenneman et al., 1985).

The plastic cores were marked at 2 cm interval, dividing each core into 5 sections. Each section was then cut by passing the core through a hot nichrome wire. The contents of each section were placed in 2 ml of sterile phosphate buffer and mixed by vortexing for 1 min. Similarly, the entire contents of glass cores were removed using 5 ml of buffer. The liquid fraction was analyzed for the number of viable cells, substrate concentrations, and fermentation end products. The galactose concentration was measured enzymatically (Boehringer Manheim GmbH). The type and amount of short chain monocarboxylic fatty acids was determined by high pressure liquid chromatography using an ion exclusion column (Amos and McInerney, 1989).

5.3 Results

Penetration rate of the cells : $E.coli$ RW262 penetrated nutrient-saturated, sand-packed cores (both glass and plastic) at a rate of 0.4 cm/h. The pore volume of 10-cm long, plastic cores was 6 ml.The distribution of the pore liquid was such that the two end sections had pore volumes of 1.5 ml each while the middle three sections had pore volumes of 1.0 ml each. Two ml of buffer was used to wash out the contents of each section. This resulted in a 1:2 dilution in the contents of three middle sections and one to one and a third dilution of the contents of the two end sections. The pore volume of 8 cm long glass cores was 5 ml and a dilution of 1:1 was obtained when 5 ml of buffer was used to extract the contents of the core. The permeability (k) of both the glass and plastic cores ranged from 7- to 7.5 Darcies .

Growth rates in broth versus porous medium : The culture used for inoculation of the cores was in the exponential phase of growth and had a cell concentration of 2×10^5 cells/mL. Since 0.1 ml of this culture was inoculated into each 8 cm long glass cores, the initial cell density used to inoculate the cores was 2×10^4 cells/ml. Immediately after the inoculation, 3.0×10^4 cells/mL were recovered, indicating that the cells did not adsorb to the sand grains. The cell concentration in duplicate cores was determined at 6,10.5, 15, 20, 35, and 41.5 h of incubation. Figure 5.1

shows that the cell population inside the core increased exponentially with a doubling time of 2 h (specific growth rate of 0.35). However, under similar experimental conditions, the doubling time of this strain in GNM broth was 1 h (specific growth rate of 0.69). Further, the lag-phase in porous media was 6 h compared to 2.5 h in broth. This suggest that the growth of the strain was restricted in sand-packed cores.

Figure 5.2 shows the change in the concentration of substrates and products in cores at different time intervals. After 41.5 h of incubation, 4.8 mM galactose was consumed and 7.4 mM acetate was produced by strain RW262 inside the core. Acetate was the only fermentation acid detected in the cores . Surprisingly, no metabolic activity, as evidenced by galactose consumption or acetate production, was detected till 20 h of incubation even though the cell density increased from 3 x 10^4 cell/mL to 4 x 10^6 cells/mL (Fig.5.1). Similarly, in liquid culture, 3.6 mM acetate was formed after a 3-fold increase in cell concentration. However, it is possible that a small amount of galactose was used which would not be detected by our assay . Another possibility was that the sand contained organic compounds which could support growth. However, when galactose was deleted from the medium used to saturate the cores, no change in cell numbers was observed. Thus, it appears that if cell densities are low (< 10^7 cells/mL), small amounts of substrate will support a large increase in the cell population .

Mechanism of cell propagation through porous medium : Figure 5.3 shows how cells moved through the core. After six hours, viable cells were detected in only the front two sections of the cores. With continued incubation, the presence of viable cells was sequentially detected in the remaining sections . As the cells propagated through the core, high cell concentrations were detected in each new section . This indicated that the cells were moving in a band-like fashion rather than dispersing through the core in a random manner.

The concentration of acetate (Fig. 5.4) and galactose (Fig.5.5) were determined in different sections of the core with time. The increase in acetate concentration in the first section during the first 15 h of incubation showed that most of the metabolic activity occured in this section. This is also where the highest cell

59

concentrations were observed (Fig.5.3). After 25 h of incubation, active metabolism, as evidenced by acetate production, was sequentially observed in the other sections of the core. Interestingly, the data showed that cell propagation proceeded the depletion of galactose or an accumulation of large amounts of acetate in a section. Thus, the cells were migrating before a substrate gradient had been generated.

5.4 Discussion

Methods have been developed to determine the in situ growth and metabolism of microorganisms in subsurface materials. Analyses showed that $E.coli$ grew at a slower rate in porous material compared to its rate of growth in liquid medium under identical experimental conditions. This shows that growth was restricted by the smaller pore spaces found in subsurface materials. The metabolism of galactose by $E. coli$ was not altered. Galactose was fermented primarily to acetate when $E. coli$ was grown in liquid culture or in sand-packed cores. Interestingly, over a 2-fold increase in cell concentration was observed before a significant change in galactose concentration was detected. This suggests that the cells are very efficient in converting small amounts of substrate into cellular material.

The concentration of cells in different sections of the core was determined with time. These data showed that cells propagated through the core in an ordered rather than a random fashion. Large amounts of galactose were detected in all core sections up to 34 h of incubation. Breakthrough of the cells occured within about 25 h of incubation. Thus, the movement of cells did not occur in response to limiting substrate concentrations.

This work shows that we can accurately determine the primary dependent variables needed to access the accuracy of mathematical models. We will also be able to determine the efficiency of growth and nutrient utilization by microorganisms in porous material. These data are needed to calculate the amounts of nutrients and time required for microbially enhanced oil recvory processes.

60

5.5 Conclusions

a. Methods have been developed to accurately determine the primary dependent variables needed to access the accuracy of mathematical models.

b. *E.coli* grew at a slower rate in porous medium compared to its rate of growth in liquid medium under indentical experimental conditions.

c. The metabolism of galactose by *E.coli* was not altered in the porous medium. Galactose was fermented primarily to acetate when *E.coli* was grown in liquid culture or in sand-packed cores.

d. The bacterial cells moved and grew throughout the available pore volume in an ordered rather than random fashion.

e. The breakthrough of cells occured before appreciable consumption of galactose or accumulation of acetate.

References

Amos, D.A., and M. J. McInerney. 1989. Poly-*B*-hydroxyalkanoate in *Syntrophomonas wolfie* Arch. Microbiol. 152: 172-177

Balch, W. E., and R. S. Wolfe. 1976. New approach to the cultivation of methanogenic bacteria:2-mercaptoethanesulfonic acid (HS-CoM)- dependent growth of *Methanobacterium ruminantium* in a pressurized atmosphere. Appl. Environ. Microbiol. 32:781-791

Coraoiciogla, M.Y., and A. Haridas. 1984.Transport and fate of microorganisms in porous media : a theoretical investigation. J.Hydrol. (Wellington North) 72:149-169

Keswick, B. H., D. S. Wang, and C. P. Gerba.1982. The use of microorganisms as groundwater tracers : a review. Ground Water , 20:142-149

Jenneman, G. E., M. J. McInerney, and R. M. Knapp.1985.Microbial penetration through nutrient-saturated Berea sand-stone. Appl. Environ. Microbiol. 50:383-391

McInerney, M. J., M. P. Bryant, and N. Pfening. 1979. Anaerobic bacterium that degrades fatty acids in syntrophic association with methanogens. Arch. Microbiol. 122:129-135.

Pfeffer, J. T. 1980. Anaerobic digestion processes, p. 187-203. *In* D. A. Stafford, B. I. Wheatley, and D. E. Hughes (ed.) Anaerobic Digestion. Applied Sciences Publishers Ltd. , London.

Reynolds, P. J., P. Sharma, G. E. Jenneman,and M. J. McInerney.1989. Mechanisms of Microbial Movement in Subsurface Materials. Appl. Environ. Microbiol. 55:2280-2286
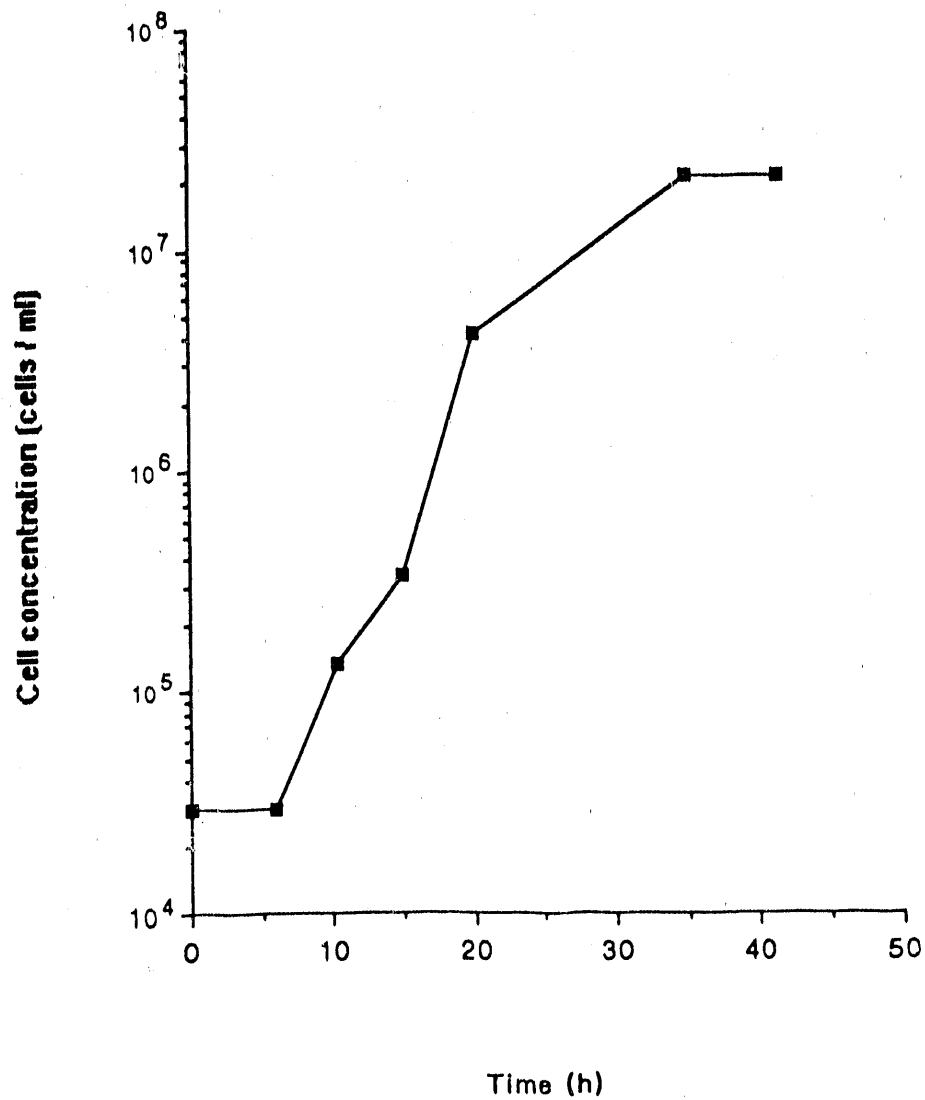
Figure 5.1 . Growth of *E . coli* RW262 in nutrient-saturated , sand-packed cores . At each time interval , the entire contents of a 8cm-long sand-packed cores were removed and the cell concentration was determined . Values are means of duplicate cores .
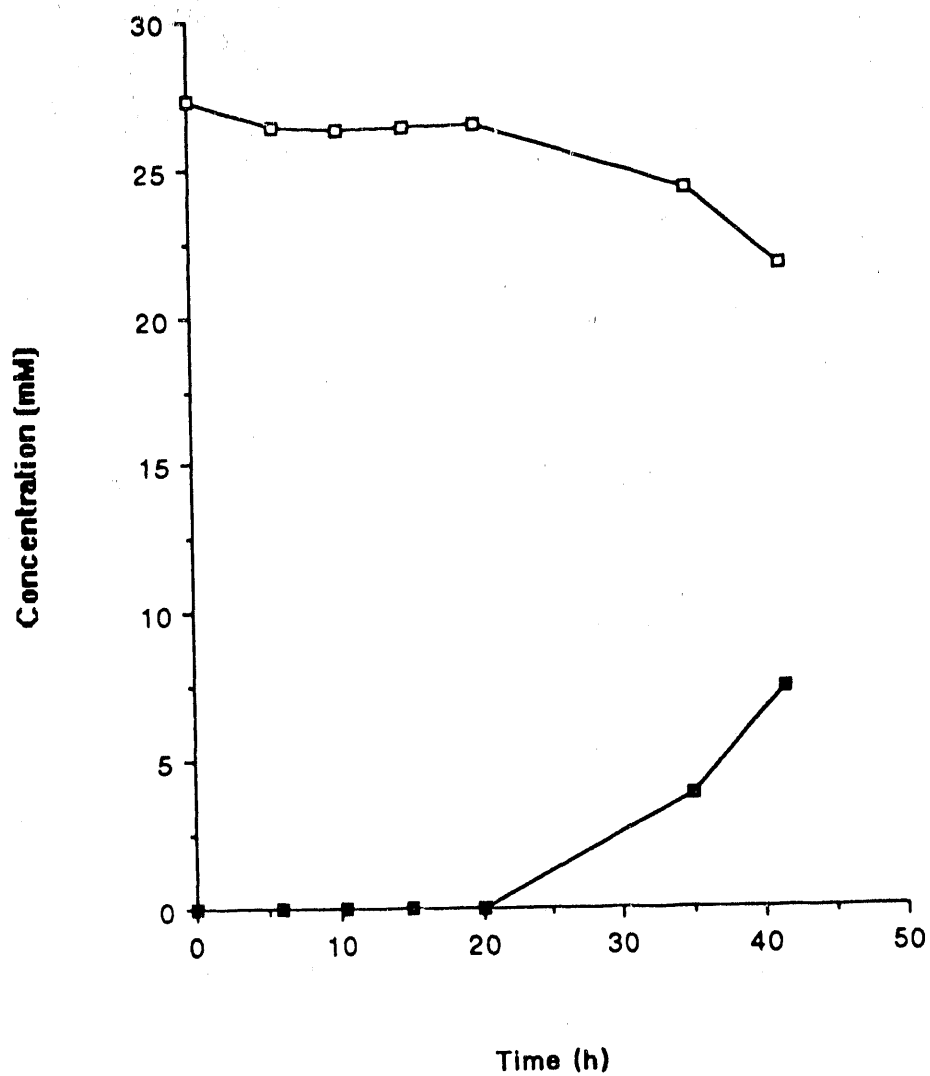
Figure 5. 2 . Change in galactose (open square) and acetate (closed square) in nutrient-saturated, sand-packed cores . The concentrations of these compounds were determined from the contents of cores used in Figure 1 .
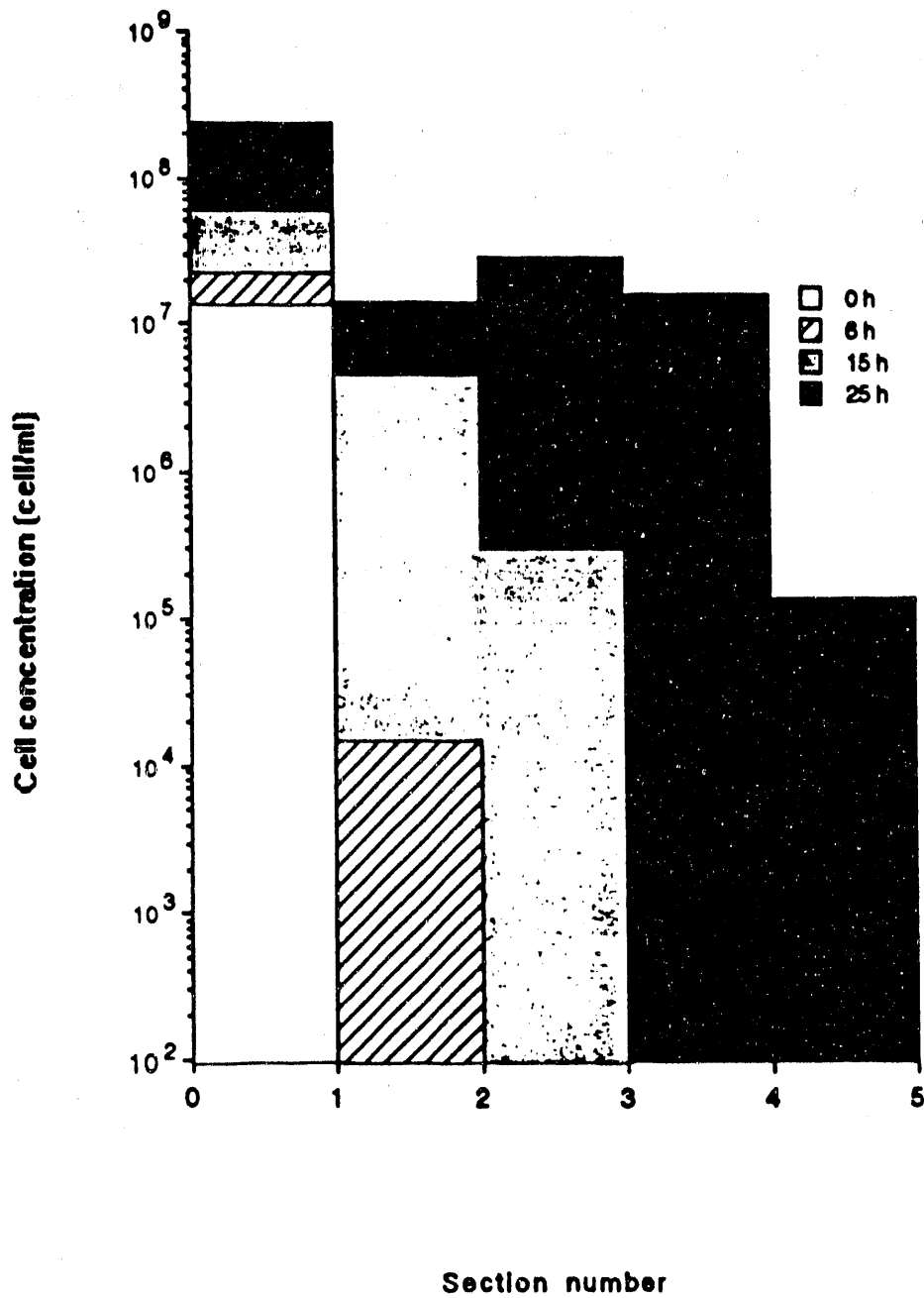
Figure 5. 3 . Propagation of cells through sand packed cores . Duplicate 10cm-long plastic cores were cut into 5 sections of equal length. The contents were removed and numbers of viable cells were determined . The detection limit was 300 cells/ml .

Figure 5.4 . Change in acetate concentration with time in different sections of the core. The concentration of acetate in each section obtained from the cores used in Figure 3 were determined.

Figure 5.5 . Change in galactose concentartion with time in the different sections of the core .
See legends of Figure 3 and 4 for details .

6. MATHEMATICAL MODELLING OF MEOR PROCESS
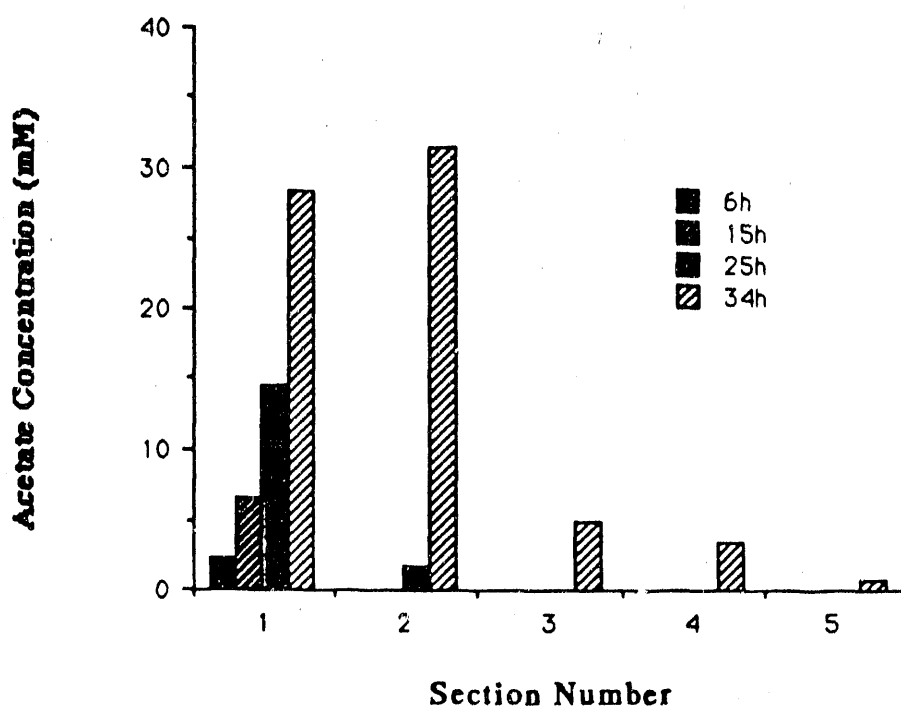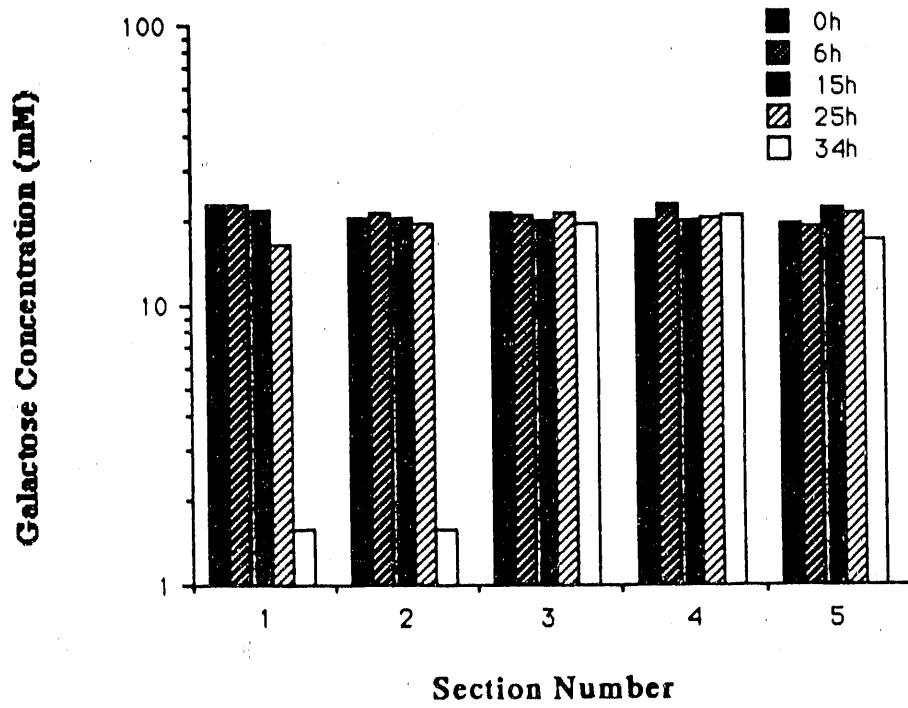
6.1 Introduction

Several selective plugging techniques have been developed [Breston, 1957] to modify permeability variations which detrimentally influence oil recovery efficiency. Unfortunately, their success is limited in stratified reservoirs. However, a microbiological approach to enhancement of oil recovery (MEOR), as an emerging technology, seems superior in many respects.

Many experimental studies [Jang, et al.,1984, Jenneman, et al., 1988, Jenneman,, et al., 1984] have been conducted to investigate MEOR processes including (1) the transportation of viable bacteria and nutrients into high permeability regions of the reservoir; (2) the in situ growth and metabolism in porous media; (3) effects of bioproducts on MEOR processes.

Associated with laboratory work, mathematical simulation has been introduced [Knapp, et al., 1988] to help understand mechanisms involved in MEOR processes. With application of physical principles from fluid dynamics and microbial process kinetics, mathematical modelling of MEOR processes are characterized by a transport-dispersion-metabolism phenomena.

This study, based on the previous work [Knapp, et al., 1988], is aimed at investigating the quantitative relationships among the species involved in the MEOR process and the permeabilty reduction as a result of this process. A three-phase, seven-species, one-dimension model is proposed. The model is specified into three categories according to the different mechanisms and flow patterns among the injection, incubation, and continued-injection processes forming a typical experimental treatment. Third-order

upwinding convective differencing scheme is adopted as a solution technique highly resistant to numerical dispersion and oscillation. Varying time step sizes implemented in computation of incubation process leads to effective enhancement of simulator efficiency.

The model was simplified to a one-phase system to simulate batch-fermentation. Numerical solutions are presented to show quantitative relationship among species during metabolism.

6.2 Microbial Activities

Materials used in a parallel experimental study are bacteria ($CH_{1.8}O_{0.5}N_{0.2}$), glucose ($C_6H_{12}O_6$), and ammonium nitrate (NH_4NO_3). There are two types of basic reactions involved in the experiments. One is anaerobic cell growth and metabolism by consumption of both glucose (carbon source) and ammonium (nitrogen source) [Bu'lock and Kristiansen,1984]:

$$C_6H_{12}O_6 + 1.2NH_4^+ \rightarrow 6CH_{1.8}O_{0.5}N_{0.2} + 3H_2O \qquad (6.1)$$
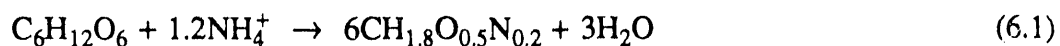
Another is growth-associated production of acetate (CH_3COO^-), carbon dioxide (CO_2), and nitrogen (N_2):

$$5C_6H_{12}O_6 + 8NO_3^- \rightarrow 10CH_3COO^- + 10CO_2 + 4N_2 + 14H_2O + 2H^+ \qquad (6.2)$$
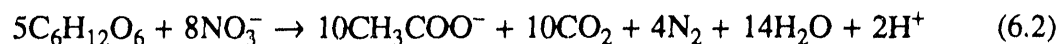
There are six species primarily involved in microbial activities: glucose ($C_6H_{12}O_6$), ammonium nitrate (NH_4NO_3), biomass ($CH_{1.8}O_{0.5}N_{0.2}$), acetate

(CH_3COO^-), carbon dioxide (CO_2), and nitrogen (N_2). However, since ammonium nitrate is separated into (1) ammonium serving as the nitrogen source for metabolism and (2) nitrate which is reduced to N_2, seven species actually go into the microbial reactions. These species, as independent variables, can be quantitatively described by appropriate mathematical formula except for CO_2, which can be estimated from the production of acetate according to the chemical balance described by Eq (6.2).

Assumptions

A set of fundamental assumptions were made to develope the model equations.

1. One-dimensional, horizontal, and linear flow. Gravity is ignored.

2. Homogeneous, isotropic, and incompressible porous medium.

3. Three-phase and Newtonian fluids: oil, water, and gas.

4. Isothermal processes are assumed for microbial transport, growth, and metabolism.

5. Both glucose and ammonium nitrate are limited.

6. Bacteria in the core are divided into cells suspended in the flowing water phase and a sessile phase composed of the cells retained on the pore surfaces.

7. Nutrients suspended in the flowing phase are assumed to fully penetrate and saturate the sessile phase so that anaerobic microbial growth and metabolism occur in the same fashion in both flowing water and sessile phases.

8. The seven species involved in metabolism are glucose (substrate 1), ammonium (positive-ion part of substrate 2), nitrate (negative-ion part of substrate 2), biomass (product 1), acetate (product 2), carbon dioxide (product 3), and nitrogen (product 4).

6.3 Model Equations

<u>Conservation Equations for Species</u>

The transport of each species suspended in the flowing water phase is governed by a typical convection-dispersion equation:

$$\frac{\partial(\phi C_i)}{\partial t} = -\frac{\partial(u_f C_i)}{\partial x} + \frac{\partial}{\partial x}(\phi K_D \frac{\partial C_i}{\partial x}) \tag{6.3}$$

where, u_f is Darcy flux, K_D is dispersion coefficient, ϕ is updated porosity, R_i is rate of generation or consumption of individual species.

Eq (6.3) is individually applied to species such as acetate (A), biomass (B), N_2 (N), glucose (S1), ammonium (S2$^+$), and nitrate (S2$^-$). However, the production of CO_2 (C) can be estimated according to acetate generation:

$$\frac{\partial C_C}{\partial t} = \omega \frac{\partial C_A}{\partial t}, \qquad \omega = \frac{(MW)_C}{(MW)_A} \tag{6.4}$$

where, C_C and C_A are respectively concentrations for CO_2 and acetate, $(MW)_C$ and $(MW)_A$ are molecular weights for CO_2 and acetate, respectively.

The accumulation of biomass attached to the pore surfaces is assumed to be the net result of biomass retention, detachment, and growth:

$$\frac{\partial}{\partial t}(\rho_B \sigma) = R_r - R_d + R_{Bs} \tag{6.5}$$

where, R_r, R_d, and R_{Bs} are rates for retention, detachment, and growth, respectively, ρ_B

is the density of biomass, and σ is the fraction of pore space occupied by retained cells.

Rate Equations for Species

The biomass retention rate is considered to be proportional to the biomass $u_f C_B$ entering a given area and to the applicable plugging capacity $(1-\sigma)\rho_B$ of the porous medium [Cernansky and Siroky, 1985]:

$$R_r = K_r(u_f C_B)(1 - \sigma)\rho_B \qquad (6.6)$$

where, K_r is the kinetic coefficient of retention, u_f is the Darcy flux, C_B is the mass concentration of biomass in the flowing phase, and σ is the updated volume fraction of the sessile phase.

The biomass detachment rate is a function of the biomass $(\sigma\rho_B)$ attached on the pore surfaces and the shear force $(\mu_f \frac{\mu_w}{K})$ between the stream of the suspension and the retained cell bodies [Cernansky and Siroky, 1985]:

$$R_d = K_d (\sigma\rho_B) u_f \frac{\mu_w}{K} \qquad (6.7)$$

where, K_d is the kinetic coefficient of detachment, K is the updated permeability, which is defined as:

$$K_f = K_0 (\frac{\phi}{\phi_0})^3, \qquad \phi = \phi_0 (1-\sigma) \qquad (6.8)$$

72

where, K_0 and ϕ_0 are respectively initial permeability and porosity.

The growth rate R_{Bs} for retained biomass, limited by availability of the two substrates (glucose and ammonium nitrate), can be easily written [Bu'lock and Kristiansen, 1984]:

$$R_{Bs} = u_{m,B} \frac{C_{S1}}{K_{B/S1} + C_{S1}} \frac{C_{S2^+}}{K_{B/S2^+} + C_{S2^+}} (\sigma \rho_B) \qquad (6.9)$$

where, C_{S1} and C_{S2^+} are mass concentrations for glucose and ammonium, respectively, $K_{B/S1}$ and $K_{B/S2^+}$ are saturation constants for biomass growth by consumption of glucose and ammonium.

Biomass generation in the flowing water phase is considered a dynamic balance of various mass exchange processes including bacterial growth, retention, and detachment:

$$R_B = R_{Bf} - R_r + R_d \qquad (6.10)$$

where, R_r and R_d are biomass retention and detachment rates, described in Eqs (6.6) and (6.7); and R_{Bf} is the growth rate for bacterial cells in the flowing phase [Bu'lock and Kristiansen, 1984]:

$$R_{Bf} = u_{m,B} \frac{C_{S1}}{K_{B/S1} + C_{S1}} \frac{C_{S2^+}}{K_{B/S2^+} + C_{S2^+}} C_B \qquad (6.11)$$

here, C_B is the concentration of bacterial cells in the flowing phase.

The production rate for acetate, carbon dioxide, and nitrogen are respectively given [Bajpai and Reuss, 1982]:

$$R_A = \begin{cases} 0, & \text{if } C_{S1} \leq C_{S1}^* \\ \mu_{mA} \dfrac{C_{S1} - C_{S1}^*}{K_{A/S1} + C_{S1} - C_{S1}^*}(C_B + \sigma\rho_B), & \text{if } C_{S1} > C_{S1}^* \end{cases} \qquad (6.12)$$

$$R_N = \begin{cases} 0, & \text{if } C_{S2} \leq C_{S2}^* \\ \mu_{mN} \dfrac{C_{S2^-} - C_{S2}^*}{K_{N/S2^-} + C_{S2^-} - C_{S2}^*}(C_B + \sigma\rho_B), & \text{if } C_{S2^-} > C_{S2}^* \end{cases} \qquad (6.13)$$

where, R_A and R_N are production rates for acetate and nitrogen, respectively; μ_{mA} and μ_{mN} are respectively maximum specific production rates for acetate and nitrogen; $K_{A/S1}$ is the saturation constant for production of acetate by consumption of glucose; $K_{N/S2^-}$ is the saturation constant for net production of nitrogen by consumption of nitrate, C_{S1}^* and C_{S2}^* are critical concentrations of glucose and ammonium nitrate, respectively. The production rate of CO_2 is proportional to that of acetate:

$$R_C = \omega R_A \qquad (6.14)$$

A typical substrate consumption equation can be used to describe the utilization of glucose and ammonium nitrate [Bu'lock and Kristiansen, 1984]:

$$R_{S1} = -\frac{1}{Y_{B/S1}}(R_{Bf} + R_{Bs}) \qquad (6.15)$$

$$R_{S2^+} = -\frac{1}{Y_{B/S2^+}}(R_{Bf} + R_{Bs}) \qquad (6.16)$$

$$R_{S2^-} = - \frac{1}{Y_{N/S2^-}} R_N \tag{6.17}$$

where, R_{S1}, R_{S2^+}, and R_{S2^-} are consumption rates of glucose, ammonium, and nitrate, respectively; $Y_{B/S1}$ and $Y_{A/S1}$, are yield coefficients for biomass and acetate per unit glucose, $Y_{B/S2^+}$ and $Y_{N/S2^-}$ are yield coefficients for biomass per unit ammonium and nitrogen per unit nitrate, respectively; and m_{S1} and m_{S2} are coefficients for energy maintenance by consumption of glucose and ammonium nitrate, respectively.

Multiphase-Flow Equations

After significant microbial plugging and biogenic gas production, the simultaneous flow of oil, water, and gas phases can occur in the porous medium during continued-injection. A three-phase transport model should be developed to describe this process.

Consider linear horizontal flow. If capillary pressure is neglected, and the gas is assumed to dissolve in both oil and water phases, a complete set of equations for pressure and saturations along the one-dimensional core system can be derived after an appropriate arrangement [Fanchi, et al., 1982]:

$$\phi C_t \frac{\partial p}{\partial t} = \beta_o \frac{\partial}{\partial x}(\psi_o \frac{\partial p}{\partial x}) + \beta_w \frac{\partial}{\partial x}(\psi_w \frac{\partial p}{\partial x}) + \beta_g[\frac{\partial}{\partial x}(\psi_g \frac{\partial p}{\partial x}) + q_g]$$
$$+ \phi \frac{\partial \sigma}{\partial t} \tag{6.18}$$

$$\frac{\partial}{\partial t}(\phi \frac{S_o}{B_o}) = \frac{\partial}{\partial x}(\psi_o \frac{\partial p}{\partial x}) \tag{6.19}$$

$$\frac{\partial}{\partial t}(\phi \frac{S_w}{B_w}) = \frac{\partial}{\partial x}(\psi_w \frac{\partial p}{\partial x}) \qquad (6.20)$$

$$\frac{\partial}{\partial t}[\phi(\frac{S_g}{B_g} + \frac{R_{so}S_o}{B_o} + \frac{R_{sw}S_w}{B_w})] = \frac{\partial}{\partial x}(\psi_g \frac{\partial p}{\partial x}) + q_g \qquad (6.21)$$

where:

$$\beta_o = B_o - R_{so}B_g, \quad \beta_w = B_w - R_{sw}B_g, \quad \beta_g = B_g \qquad (6.22)$$

$$\psi_o = \frac{K\lambda_o}{B_o}, \quad \psi_w = \frac{K\lambda_w}{B_w}, \quad \psi_g = K(\frac{\lambda_g}{B_g} + \frac{R_{so}\lambda_o}{B_o} + \frac{R_{sw}\lambda_w}{B_w}) \qquad (6.23)$$

$$\lambda_o = \frac{K_{ro}}{\mu_o}, \quad \lambda_w = \frac{K_{rw}}{\mu_w}, \quad \lambda_g = \frac{K_{rg}}{\mu_g} \qquad (6.24)$$

$$q_g = \frac{1}{\rho_{CS}}\frac{\partial C_C}{\partial t} + \frac{1}{\rho_{NS}}\frac{\partial C_N}{\partial t} \qquad (6.25)$$

$$C_t = C_oS_o + C_wS_w + C_gS_g \qquad (6.26)$$

$$C_o = -\frac{1}{B_o}\frac{\partial B_o}{\partial p} + \frac{B_g}{B_o}\frac{\partial R_{so}}{\partial p} \qquad (6.27)$$

$$C_w = -\frac{1}{B_w}\frac{\partial B_w}{\partial p} + \frac{B_g}{B_w}\frac{\partial R_{sw}}{\partial p} \qquad (6.28)$$

$$C_g = -\frac{1}{B_g}\frac{\partial B_g}{\partial p} \tag{6.29}$$

$$\phi = \phi_0(1-\sigma), \quad K = K_0\left(\frac{\phi}{\phi_0}\right)^3 \tag{6.30}$$

$$S_o + S_w + S_g + \sigma = 1 \tag{6.31}$$

where, p is pressure; S_o, S_w, and S_g are saturations for oil, water, and gas respectively; B_o, B_w, and B_g are respectively formation volume factors for oil, water, and gas; K_{ro}, K_{rw}, and K_{rg}, are relative permeabilities to oil, water, and gas; μ_o, μ_w, and μ_g are viscosities for oil, water, and gas; C_t is total compressibility, C_o, C_w, and C_g are compressibilities for oil, water, and gas phases, respectively, q_g is the total gas production (including CO_2 and N_2) generated as a result of metabolism; ρ_{CS} and ρ_{NS} are respectively densities of CO_2 and N_2 at standard conditions.

6.4 Simplification and Specification

Let μ_{ss} be the specific growth rate for biomass in the two-substrate system:

$$\mu_{ss} = \mu_{m,B}\frac{C_{S1}}{K_{B/S1} + C_{S1}}\cdot\frac{C_{S2^+}}{K_{B/S2^+} + C_{S2^+}} \tag{6.32}$$

thus, the sessile biomass balance equation (6.5) can be simplified:

$$\frac{\partial \sigma}{\partial t} = K_r u_f C_B(1-\sigma) - K_d u_f \mu_w \frac{\sigma}{K} + \mu_{ss}\sigma \tag{6.33}$$

since ρ_B is a constant. If the injection flux, u_f, is specified, the species equation (6.3) can be rewritten:

$$\frac{\partial C_i}{\partial t} = -\frac{u_f}{\phi}\frac{\partial C_i}{\partial x} + \frac{1}{\phi}\frac{\partial}{\partial x}(\phi K_D \frac{\partial C_i}{\partial x}) + \phi_0 C_i \frac{\partial \sigma}{\partial t} + R_i \qquad (6.34)$$

In addition, further specifications can be made for the different mechanisms and flow patterns among the injection, incubation, and continued-injection processes.

Injection Process

Since bacterial plugging and biogenic gas production appear insignificant during initial injection, the residual oil and biogenic gas are immobile. Thus, a single flowing water phase can be assumed during this process and the pressure equation can simply expressed by Darcy's equation:

$$\frac{\partial p}{\partial x} = -u_f \frac{\mu_w}{K} \qquad (6.35)$$

where, u_f, the Darcy flux, is assumed to be a constant; μ_w is viscosity of the water phase; and K is the updated permeability.

In addition, since microorganisms and nutrients are transported into the core system during an injection period much shorter than incubation time, it is assumed that growth and metabolism occur only in the flowing phase during injection. Therefore, growth, production, and consumption rates by the sessile bacterium phase during injection are neglected in the pertinent equations. A specified model with appropriate initial and boundary conditions is proposed for this process, as shown in the Table 6.1.

Incubation Process

The sandstone core is "shut-in" to allow microbial growth and metabolism in this process. Since there is no flow, the rate-controlled retention and detachment terms disappear from Eq (6.33), and the convection terms are dropped from the convection-dispersion Eq (6.34). Although molecular diffusion for each species exists during incubation the molecular diffusion is much smaller compared with the species generation and consumption rates and is neglected. Under these conditions, the model is reduced to a set of zero-dimension equations applied to each grid block. Each block behaves like a single batch fermenter, with no mass exchange with adjacent blocks. This simplification offers the opportunity to increase time step sizes during the incubation computation. Pressure is assumed to be uniform along the core because no flow occurs in the core, and thus the pressure gradient terms in the pressure equation (6.18) are dropped. A simplified model for the incubation process is summarized in the Table 6.2.

Continued-injection Process

A major characteristic in this process is simultaneous flow of oil, water, and gas phases as a result of preferential microbial plugging and significant biogenic gas production. Although much of the gas may dissolve in the oil phase, some gas as a free phase may flow through own channels in the core, particularly towards the outlet from the core. The rate-controlled retention and detachment of bacteria may become active again during the continued-injection. A general three-phase and seven-species model is summarized in Table 6.3.

6.5 Numerical Solutions

The partial differential equations are solved by using the method of lines [Ames, 1977]. Spatial derivatives are approximated by their finite difference formulas while the temporal derivatives remain continuous, and the numerical solutions are carried out using the 1(2)-order Runge-Kutta-Fehlberg method.

The first-order spatial derivative corresponding to the convective transport for species i in Eq (6.34) is replaced by Leonard's [1984] third-order upwind formula which is resistant to numerical dispersion and oscillation:

$$\left[\frac{\partial C_i}{\partial x}\right]_j = \frac{(C_i)_{j-2} - 6(C_i)_{j-1} + 3(C_i)_j + 2(C_i)_{j+1}}{6\Delta x} + \theta(\Delta x^3) \qquad (6.36)$$

Since the concentration $(C_i)_0$ required in Eq (6.36) does not exist, the first-order spatial derivative at $j = 2$ is expressed by the two-point central weighting scheme:

$$\left[\frac{\partial C_i}{\partial x}\right]_2 = \frac{(C_i)_3 - (C_i)_1}{2\Delta x} + \theta(\Delta x^2) \qquad (6.37)$$

The dispersion term, a second-order spatial derivative, is approximated by the second-order central finite difference scheme:

$$\left[\frac{\partial}{\partial x}(\phi K_D \frac{\partial C_i}{\partial x})\right]_j =$$

$$\frac{(\phi K_D)_{j+\frac{1}{2}}[(C_i)_{j+1} - (C_i)_j] - (\phi K_D)_{j-\frac{1}{2}}[(C_i)_j - (C_i)_{j-1}]}{\Delta x^2} \qquad (6.38)$$

To approximate the second-order spatial derivatives in the pressure equation

(6.18), a second-order central difference scheme is used:

$$\left[\frac{\partial}{\partial x}(\psi_l \frac{\partial p}{\partial x})\right]_j = \frac{(\psi_l)_{j+\frac{1}{2}}(p_{j+1} - p_j) - (\psi_l)_{j-\frac{1}{2}}(p_j - p_{j-1})}{\Delta x^2} \qquad (6.39)$$

Consider an explicit algorithm to calculate saturations using a first-order approximation to Eq (6.19) and (6.20), respectively:

$$\frac{\left[\frac{\phi S_o}{B_o}\right]_j^{n+1} - \left[\frac{\phi S_o}{B_o}\right]_j^{n}}{\Delta t} = \left[\frac{\partial}{\partial x}(\psi_o \frac{\partial p}{\partial x})\right]_j^{n+1} \qquad (6.40)$$

$$\frac{\left[\frac{\phi S_w}{B_w}\right]_j^{n+1} - \left[\frac{\phi S_w}{B_w}\right]_j^{n}}{\Delta t} = \left[\frac{\partial}{\partial x}(\psi_w \frac{\partial p}{\partial x})\right]_j^{n+1} \qquad (6.41)$$

Through discretization in space and time, the model equations are transfered to a set of finite difference equations.

Since the incubation time is much longer than either the injection or continued-injection times, the simulator efficiency greatly depends on the time step sizes used in the incubation computation. Although bacterial cells grow at some exponential rate, growth, product formation, and substrate consumption rates decrease with time, and even become zero as the substrate is consumed. Hence, it is reasonable that the time step size be chosen to increase at an appropriate exponential rate during the incubation process.

Let Δt_0 be an initial time step size, and θ a time-step-varying factor. Thus the time step size may increase in the following manner :

$$\Delta t_n = \theta \Delta t_{n-1} = \theta^{n-1} \Delta t_0 \tag{6.42}$$

6.6 Application

An experiment of static batch fermentation in an anaeorobic, nutrient-saturated, and unconsolidated porous media has been conducted. Growth of bacterial cells, along with production of acetate, CO_2, and N_2 by consumption of galactose and ammonium nitrate, has been observed. To simulate these microbial activities, the proposed model is reduced to a zero-dimension, batch-ferementer system as shown in Table 6.4. Yield coefficients are stoichiometrically estimated from chemical balance equations (Table 6.5). Other kinetic parameters are given in Table 6.8. Experimental results are presented in Table 6.7. Results from the simulator are shown in Table 6.8.

Comparison of simulation responses with experimental results are shown in Figures 6.1 to 6.5. A good match is achieved for galactose consumption (Figure 6.1) and acetate production (Figure 6.4). Biomass growth rate (μ_B) (Figure 6.3) given by the simulator is lower than that from the experiment since growth lag-phase has not been considered in the model. Also presented are comparisons of consumption of nitrate (Figure 6.2) and N_2 production (Figure 6.5) between simulated and experimental results.

From chemical balance equations (Table 6.5), consumption of one-mole galactose should result in production of two-mole acetate, and two-mole nitrate should be reduced to one-mole N_2. The results from the simulator satisfy the mass-balance criteria above.

6.7 Conclusions

(1) A three-phase, seven species, one-dimensional model of the microbial process is proposed.

(2) A chemical balance equation describing the microbial process is used in which glucose and nitrate serve as nutrients and acetate, carbon dioxide, nitrogen and biomass are products.

(3) The model addresses three different mechanism and flow pattern catagories: initial injection, incubation, and continued injection. Material balance and multiphase flow equations are proposed for each of the catagories.

(4) A third order upwinding convective differencing scheme is adopted as a solution technique. This technique is highly resistant to numerical dispersion and oscillation.

(5) The model is successfully simplified to one-phase to simulate batch fermentation.

REFERENCES

Ames, W.F. (1977). Numerical Methods for Partial Differential Equations, 2nd ed., Academic Press, New York.

Bajpai, R.K. and M. Reuss. 1982. Coupling of mixing and microbial kinetic for evaluating the performance of bioreactors, Can. J. Chem. Eng., 60, 384-392.

Breston, J.N. 1957. Selective plugging of waterflood input wells: theory, methds and results, J. Pet. Tech. (Mar. 1957) 26-31.

Bu'lock, J. and B. Kristiansen. 1984. Basic Biotechnology, New York, 75-131.

Cernansky, A. and R. Siroky. 1985. Deep-bed filtration on filament layers of particles polydispersed in liquids, International Chemical Engineering, 25(2), 364-375.

Fanchi, J.R., K.J. Harpole, and S.W. Bujnowski. 1982. BOAST: A Three-Dimensional, Three-Phase Black Oil Applied Simulation Tool (Version 1.1), Vol.1: Technical Description and Fortran Code, Dept. of Energy DOE/BC/10033-3, USDOE Technical Information Center, Oak Ridge, Tennessee, 1-17.

Jang, L.K., M.M. Sharma, and T.F. Yen. 1984. The transport of bacteria in porous media and its significance in microbial enhanced oil recovery, Paper SPE 12770 presented at the 1984 California Regional Meeting, Long Beach, CA, (Apr. 1984) 11-13.

Jenneman, G.E., M.J. McInerney and R.M. Knapp. 1985. Microbial penetration through nutrient-saturated berea sandstone, Appl. Environ. Microbiol., 50, 383-391.

Jenneman, G.E., R.M. Knapp, M.J. McInerney, D.E. Menzie and D.E. Revus. 1984. Experimental studies of in situ microbial enhanced oil recovery, Soc. Pet. Eng. J., 24, 33-37.

Knapp, R.M., F. Civan, and M.J. McInerney. 1988. Modeling growth and transport of microorganisms in porous formations, IMACS, Proceedings of 12th World Congress on Scientific Computation, July 18-22, 1988, Paris, France, Edited by R. Vichnevetsky, P.Borne, and J. Vignes, Vol. 3, 676-679.

Leonard, B.P. 1984. Third-order upwinding as a rational basis for computational fluid dynamics, Computational Techniques and Applications: CTAC-83, Editors, J. Noye and C. Fletcher, 106-120.

Table 6.1 Model Equations for Injection Process

Types	Equations
Species	$$\frac{\partial C_i}{\partial t} = -\frac{u_f}{\phi}\frac{\partial C_i}{\partial x} + \frac{1}{\phi}\frac{\partial}{\partial x}(\phi K_D \frac{\partial C_i}{\partial x}) + \phi_0 C_i\frac{\partial \sigma}{\partial t} + R_i$$ $$\frac{\partial C_C}{\partial t} = \omega\frac{\partial C_N}{\partial t}, \quad \text{or} \quad C_C = \omega C_A$$ where , $i = A, B, N, S1, S2^+, S2^-$
Sessile	$$\frac{\partial \sigma}{\partial t} = K_r u_f C_B(1 - \sigma) - K_d \sigma u_f \frac{\mu_w}{K}$$
Pressure	$$\frac{\partial p}{\partial x} = -u_f\frac{\mu_w}{K}$$
I.C.	$$(C_i)_{t=0} = C_i^0, \quad (\sigma)_{t=0} = \sigma^0, \quad (p)_{t=0} = p^0$$
B.C.	$$\left[u_f C_i - \phi K_D\frac{\partial C_i}{\partial x}\right]_{x=0} = u_f(C_i)_{inlet}, \quad \left[\frac{\partial C_i}{\partial x}\right]_{x=L} = 0$$ $$(p)_{x=0} = p_{inj}$$

I.C. - Initial Conditions
B.C. - Boundary Conditions

Types	Equations
	Table 6.2 Model Equations for Incubation Process
Species	$$\frac{\partial C_i}{\partial t} = \phi_0 \, C_i \frac{\partial \sigma}{\partial t} + R_i$$ $$\frac{\partial C_C}{\partial t} = \omega \frac{\partial C_A}{\partial t}, \quad \text{or} \quad C_C = \omega \, C_A$$ where, i = A, B, N, S1, S2$^+$, S2$^-$
Sessile	$$\frac{\partial \sigma}{\partial t} = \mu_{ss} \sigma$$
Pressure	$$\phi C_t \frac{\partial p}{\partial t} = B_g \left(\frac{1}{\rho_{CS}} \frac{\partial C_C}{\partial t} + \frac{1}{\rho_{NS}} \frac{\partial C_N}{\partial t} \right) + \phi \frac{\partial \sigma}{\partial t}$$
I.C.	$(C_i)_{t=T_s} = (C_i)^s, \quad (\sigma)_{t=T_s} = (\sigma)^s, \quad (p)_{t=T_s} = (p)^s$

I.C. - Initial Conditions

Table 6.3 Model Equations for Continued-injection Process

Types	Equations
Species	$\dfrac{\partial C_i}{\partial t} = -\dfrac{u_f}{\phi}\dfrac{\partial C_i}{\partial x} + \dfrac{1}{\phi}\dfrac{\partial}{\partial x}(\phi K_D \dfrac{\partial C_i}{\partial x}) + \phi_0\, C_i\dfrac{\partial \sigma}{\partial t} + R_i$ $\dfrac{\partial C_C}{\partial t} = \omega\, \dfrac{\partial C_A}{\partial t}$, or $C_C = \omega\, C_A$ where , $i = A, B, N, S1, S2^+, S2^-$
Sessile	$\dfrac{\partial \sigma}{\partial t} = K_r u_f C_B(1-\sigma) - K_d\sigma u_f\dfrac{\mu_w}{K}$
Pressure	$\phi C_i\dfrac{\partial p}{\partial t} = \beta_o\dfrac{\partial}{\partial x}(\psi_o\dfrac{\partial p}{\partial x}) + \beta_w\dfrac{\partial}{\partial x}(\psi_w\dfrac{\partial p}{\partial x}) + \beta_g[\dfrac{\partial}{\partial x}(\psi_g\dfrac{\partial p}{\partial x}) + q_g]$ $\qquad\qquad + \phi\dfrac{\partial \sigma}{\partial t}$
Saturations	$\dfrac{\partial}{\partial t}(\phi\dfrac{S_o}{B_o}) = \dfrac{\partial}{\partial x}(\psi_o\dfrac{\partial p}{\partial x})$, $\dfrac{\partial}{\partial t}(\phi\dfrac{S_w}{B_w}) = \dfrac{\partial}{\partial x}(\psi_w\dfrac{\partial p}{\partial x})$ $\dfrac{\partial}{\partial t}[\phi(\dfrac{S_g}{B_g} + \dfrac{R_{so}S_o}{B_o} + \dfrac{R_{sw}S_w}{B_w})] = \dfrac{\partial}{\partial x}(\psi_g\dfrac{\partial p}{\partial x}) + q_g$
I.C.	$(C_i)_{t=T_w} = {}_i^w$, $(\sigma)_{t=T_w} = \sigma^w$, $(p)_{t=T_w} = p^w$ $(S_j)_{t=T_w} = S_j^w$, $j = o, w, g$
B.C.	$\left[u_f C_i - \phi K_D\dfrac{\partial C_i}{\partial x}\right]_{x=0} = u_f(C_i)_{inlet}$, $\left[\dfrac{\partial C_i}{\partial x}\right]_{x=L} = 0$ $(p)_{x=0} = p_{inlet}$

I.C. - Initial Conditions
B.C. - Boundary Conditions

Table 6.4 Batch-Fermentation Two-Substrate Model

Types	Equations
Biomass	$$\dfrac{dC_B}{dt} = \mu_{Bm} \dfrac{C_{S1}}{K_{B/S1} + C_{S1}} \dfrac{C_{S2'}}{K_{B/S2'} + C_{S2'}} C_B$$
Acetate	$$\dfrac{dC_A}{dt} = \mu_{Am} \dfrac{C_{S1} - C_{S1}^*}{K_{A/S1} + C_{S1} - C_{S1}^*} C_B$$
CO_2	$$C_C = \omega C_A, \quad \text{where,} \quad \omega = \dfrac{(\text{Mol. Wrt.})_C}{(\text{Mol. Wrt.})_A}$$
N_2	$$\dfrac{dC_N}{dt} = \mu_{Nm} \dfrac{C_{S2^-} - C_{S2}^*}{K_{N/S2^-} + C_{S2^-} - C_{S2}^*} C_B$$
Glucose	$$\dfrac{dC_{S1}}{dt} = -\dfrac{1}{Y_{B/S1}} \left(\dfrac{dC_B}{dt}\right) - \dfrac{1}{Y_{A/S1}} \left(\dfrac{dC_A}{dt}\right) - m_{S1} C_B$$
Ammonium	$$\dfrac{dC_{S2'}}{dt} = -\dfrac{1}{Y_{B/S2'}} \left(\dfrac{dC_B}{dt}\right) - m_{S2} C_B$$
Nitrate	$$\dfrac{dC_{S2^-}}{dt} = -\dfrac{1}{Y_{N/S2^-}} \left(\dfrac{dC_N}{dt}\right)$$
Initial Conditions	$$(C_B)_{t=0} = C_B^0, \quad (C_{S1})_{t=0} = C_{S1}^0, \quad (C_{S2})_{t=0} = C_{S2}^0$$ $$(C_A)_{t=0} = 0, \quad (C_C)_{t=0} = 0, \quad (C_N)_{t=0} = 0$$

Table 6.5 Stoichiometric Parameters

Chemical Balance	$C_6H_{12}O_6 \rightarrow 2CH_3COO^- + 2CO_2$ $2NO_3^- \rightarrow N_2$ $C_6H_{12}O_6 + 1.2NH_4^+ \rightarrow 6CH_{1.8}O_{0.5}N_{0.2}$
Molecular Weight	$C_6H_{12}O_6$ (galactose – S1) = 180.156 NH_4^+ (ammonium – S2$^+$) = 18.042 NO_3^- (nitrate – S2$^-$) = 62.01 CH_3COO^- (acetate – A) = 59.044 CO_2 (carbon dioxide – C) = 44.01 N_2 (nitrogen – N) = 28.02 $CH_{1.8}O_{0.5}N_{0.2}$ (biomass – B) = 24.6264
Yield Coefficients	$Y_{B/S1} = \dfrac{6 \times 24.6264}{1 \times 180.156} = 0.8202$ $Y_{B/S2^+} = \dfrac{6 \times 24.6264}{1.2 \times 18.042} = 6.8247$ $Y_{A/S1} = \dfrac{2 \times 59.044}{1 \times 180.156} = 0.6555$ $Y_{N/S2^-} = \dfrac{1 \times 28.02}{2 \times 62.01} = 0.2259$

Table 6.6 Kinetic Parameters for Batch Fermentation

Symbols	Definitions	Values	Units	Source Comments
μ_{Bm}	max specific growth rate for biomass	0.602	1/hr	(1)
μ_{Am}	max specific production rate for acetate	3.35	1/hr	estimated*
μ_{Nm}	max specific production rate for N_2	1.21	1/hr	estimated*
$K_{B/S1}$	saturation const for biomass on galactose	1.345	mg/cm^3	estimated*
$K_{B/S2^+}$	saturation const for biomass on NH_4^+	1.234	mg/cm^3	estimated*
$K_{A/S1}$	saturation const for acetate on galactose	0.01	mg/cm^3	estimated*
$K_{N/S2^-}$	saturation const for N_2 on NO_3^-	0.01	mg/cm^3	estimated*
$C_{S1}^\bullet$	critical concentration for galactose	0.03	mg/cm^3	(2)
$C_{S2^-}^\bullet$	critical concentration for NO_3^-	0.03	mg/cm^3	(2)
m_{S1}	coeff of energy maintenance by galactose	0.0001	mg/mg.hr	estimated*
m_{S2^-}	coeff of energy maintenance by NO_3^-	0.0001	mg/mg.hr	estimated*

* by trial and error
(1) Measured in batch growth experiment
(2) Bajpai and Reuss, 1982

Table 6.7 Experiment Results from Batch Fermentation

Time (hr)	Galactose (mM)	Nitrate (mM)	Biomass (cells/cm^3)	Acetate (mM)	CO$_2$ (mM)	N$_2$ (mM)
00.0	26.6	35.3	2.94×10^4	0.00	0.00	0.00
06.0	26.4	34.71	2.94×10^4	0.00	0.00	0.00
10.5	26.3	34.91	1.33×10^5	0.00	0.00	0.00
15.0	26.4	34.85	3.30×10^5	0.00	0.00	0.00
20.0	26.5	34.9	4.10×10^6	0.00	0.00	0.00
35.0	24.35	26.63	2.16×10^7	3.82	3.82	4.34
41.5	21.8	24.06	2.16×10^7	7.41	7.41	5.62

Table 6.8 Simulation Response to Batch Fermentation

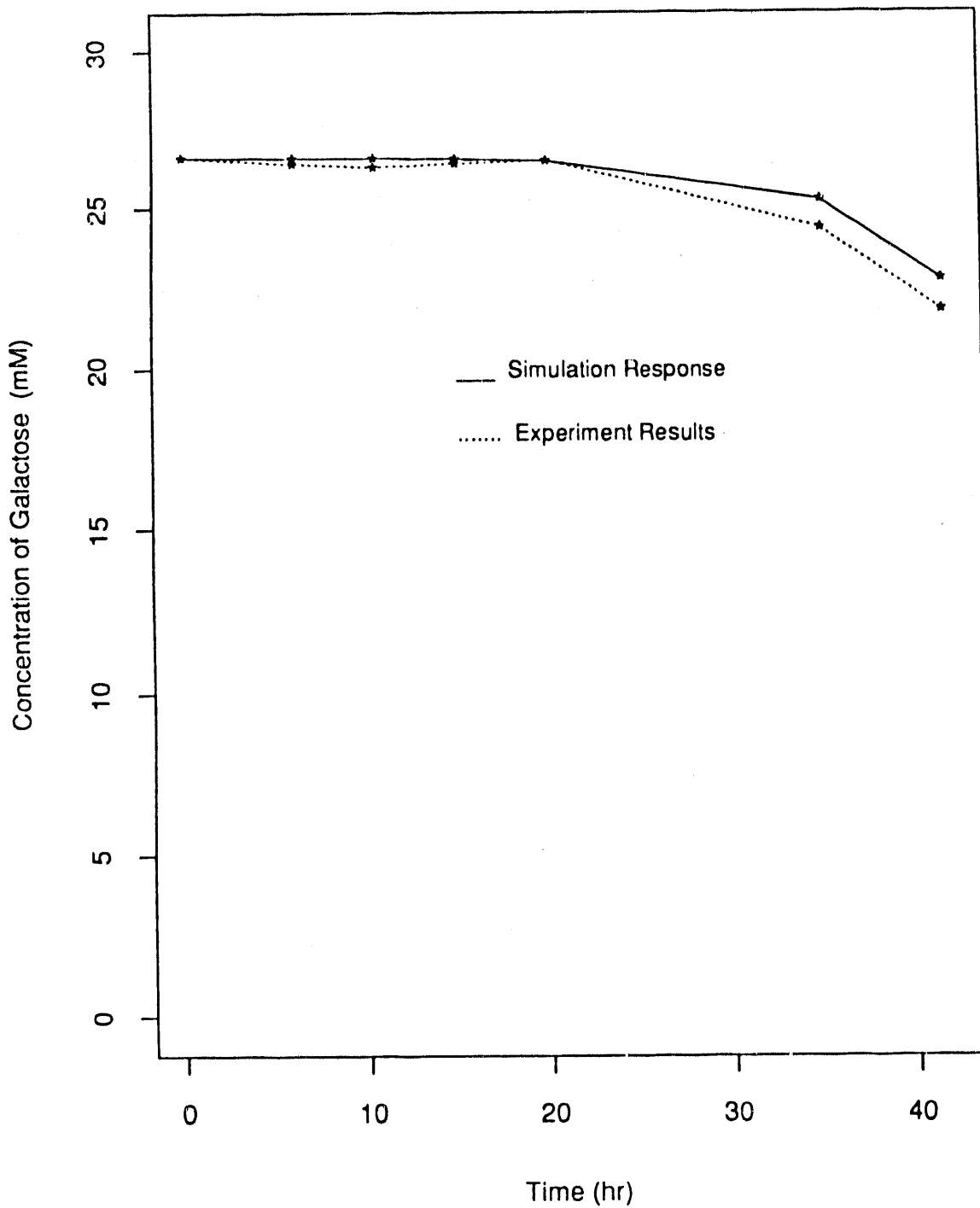| Time (hr)	Galactose (mM)	Nitrate (mM)	Biomass (cells/cm^3)	Acetate (mM)	CO$_2$ (mM)	N$_2$ (mM)
00.0	26.6	35.3	2.94×10^4	0.00	0.00	0.00
06.0	26.6	35.3	7.68×10^4	0.02	0.02	0.01
10.5	26.6	35.2	1.58×10^5	0.04	0.04	0.03
15.0	26.5	35.1	3.24×10^5	0.10	0.10	0.08
20.0	26.5	34.9	7.20×10^5	0.23	0.23	0.18
35.0	25.2	31.3	7.84×10^6	2.64	2.64	2.01
41.5	22.8	24.0	2.16×10^7	7.40	7.40	5.61

Figure 6.1 : Consumption of Galactose
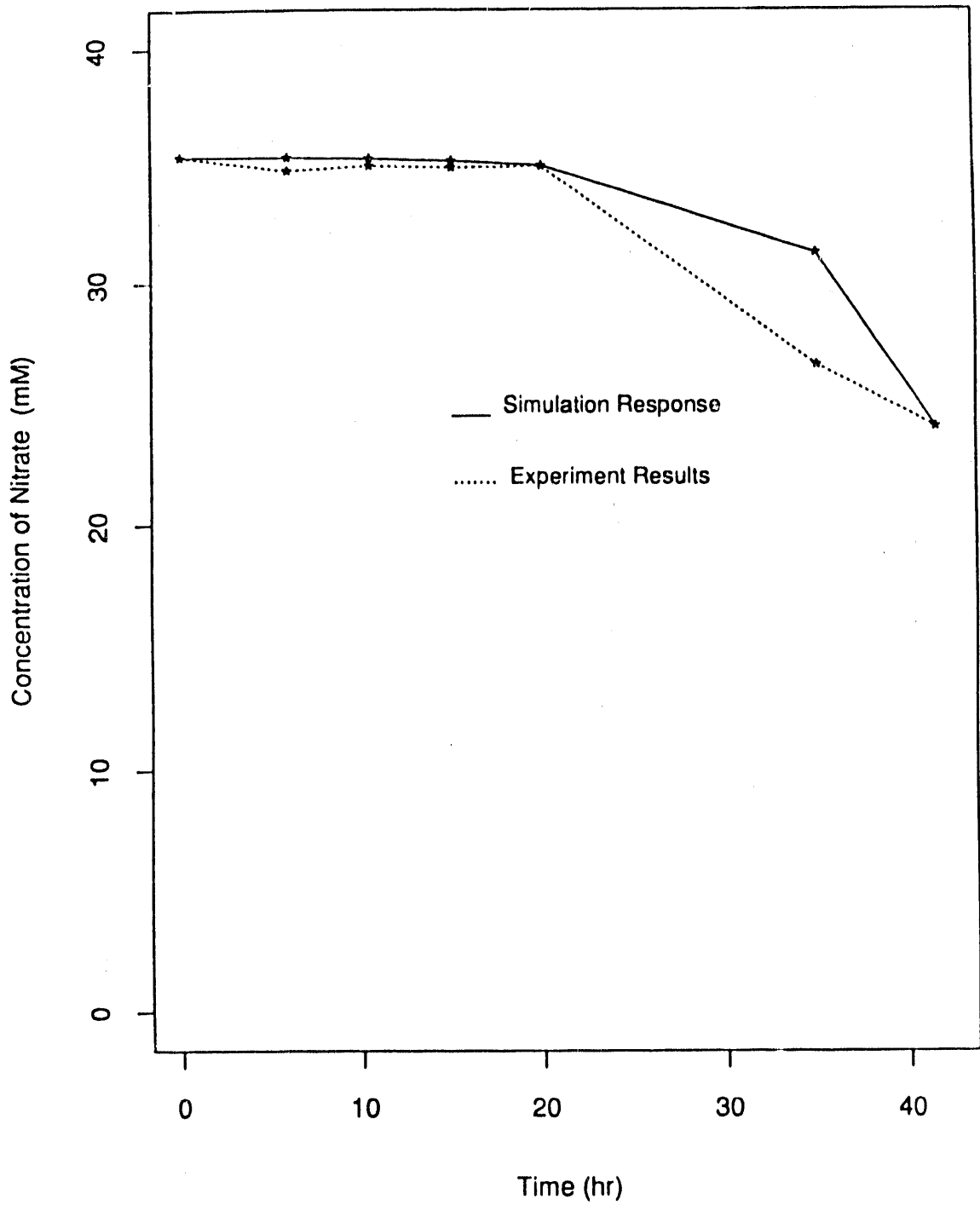during Batch Fermentation

Figure 6.2 : Consumption of Nitrate
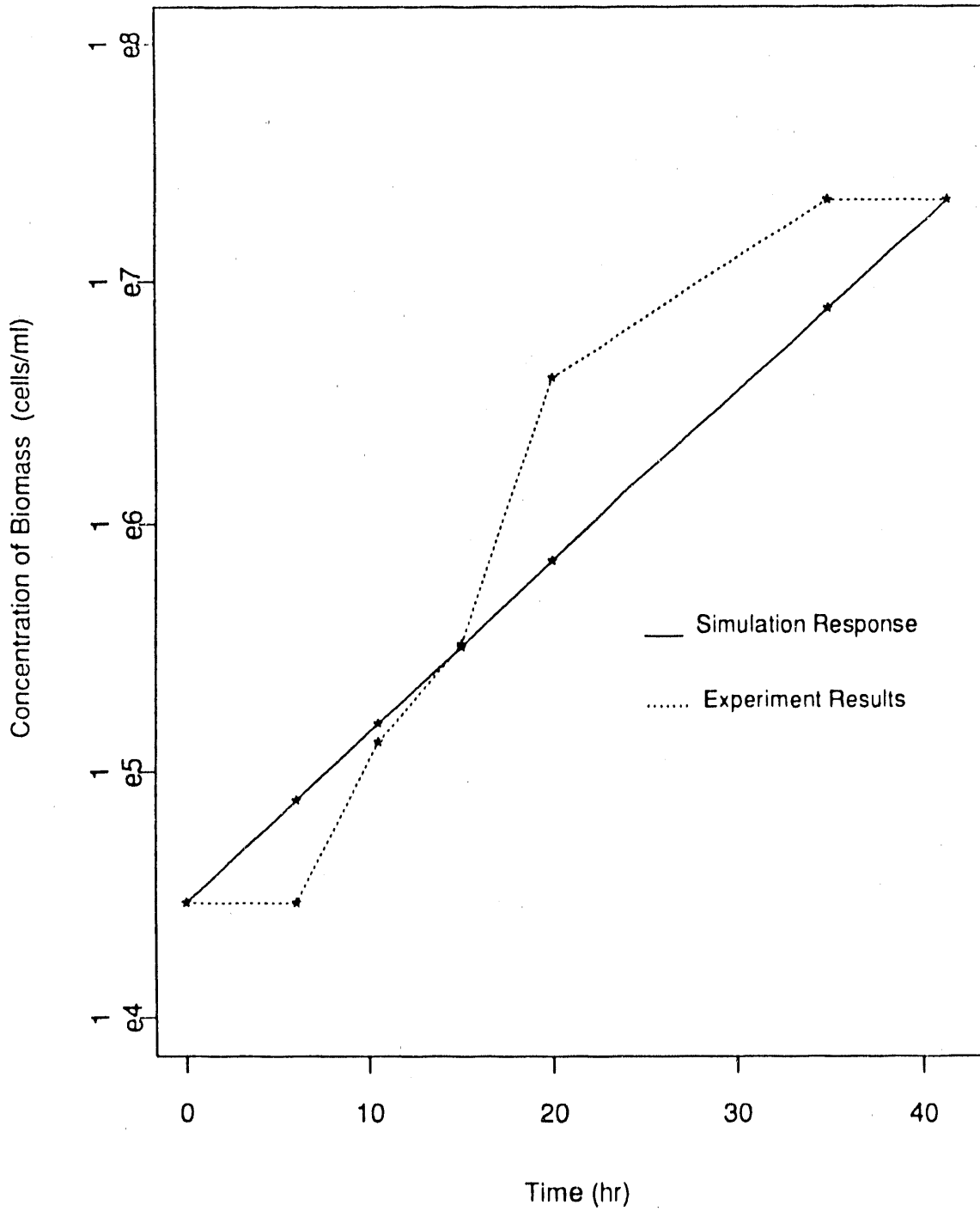during Batch Fermentation

Figure 6.3 : Growth of Biomass
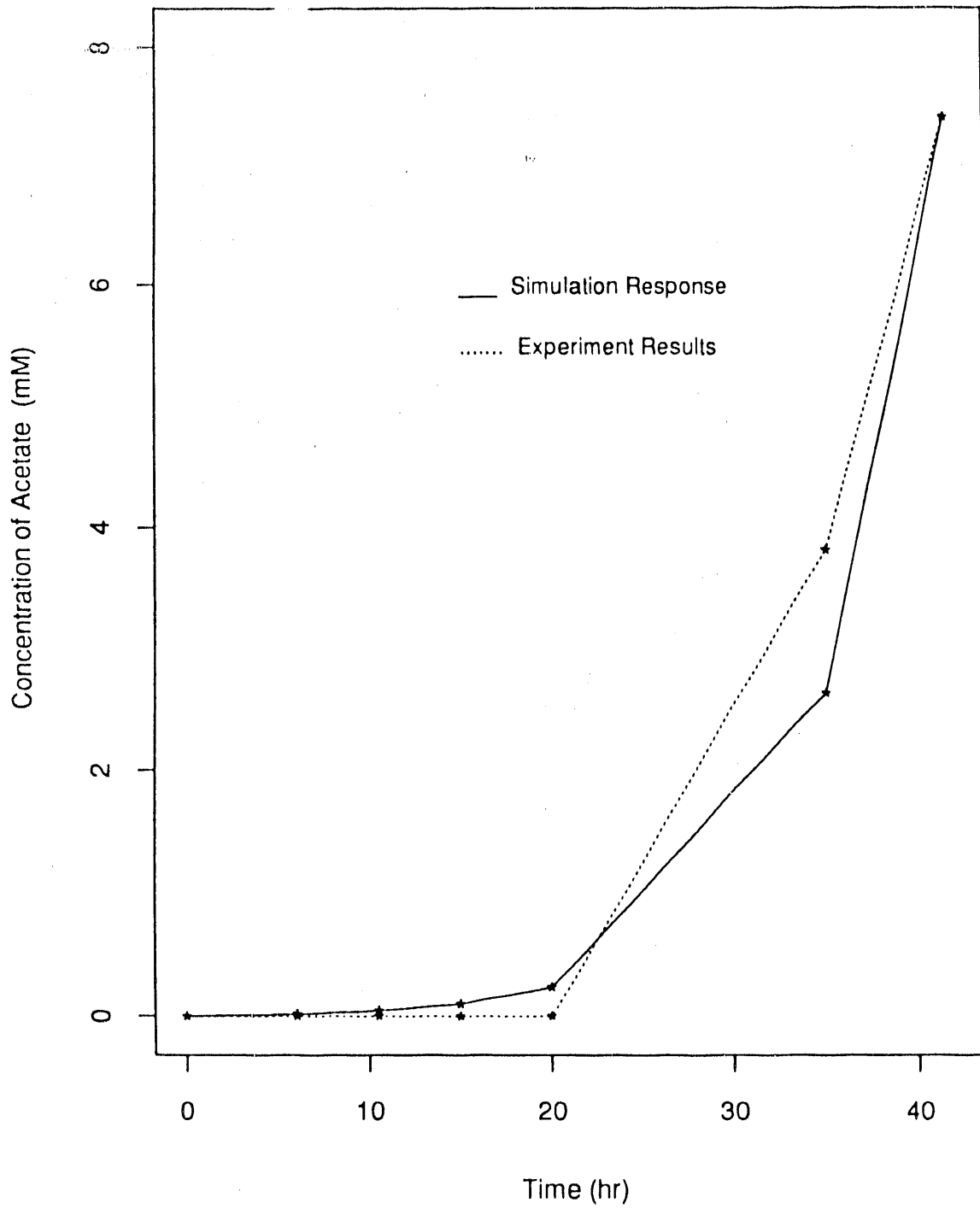during Batch Fermentation

Figure 6.4 : Production of Acetate
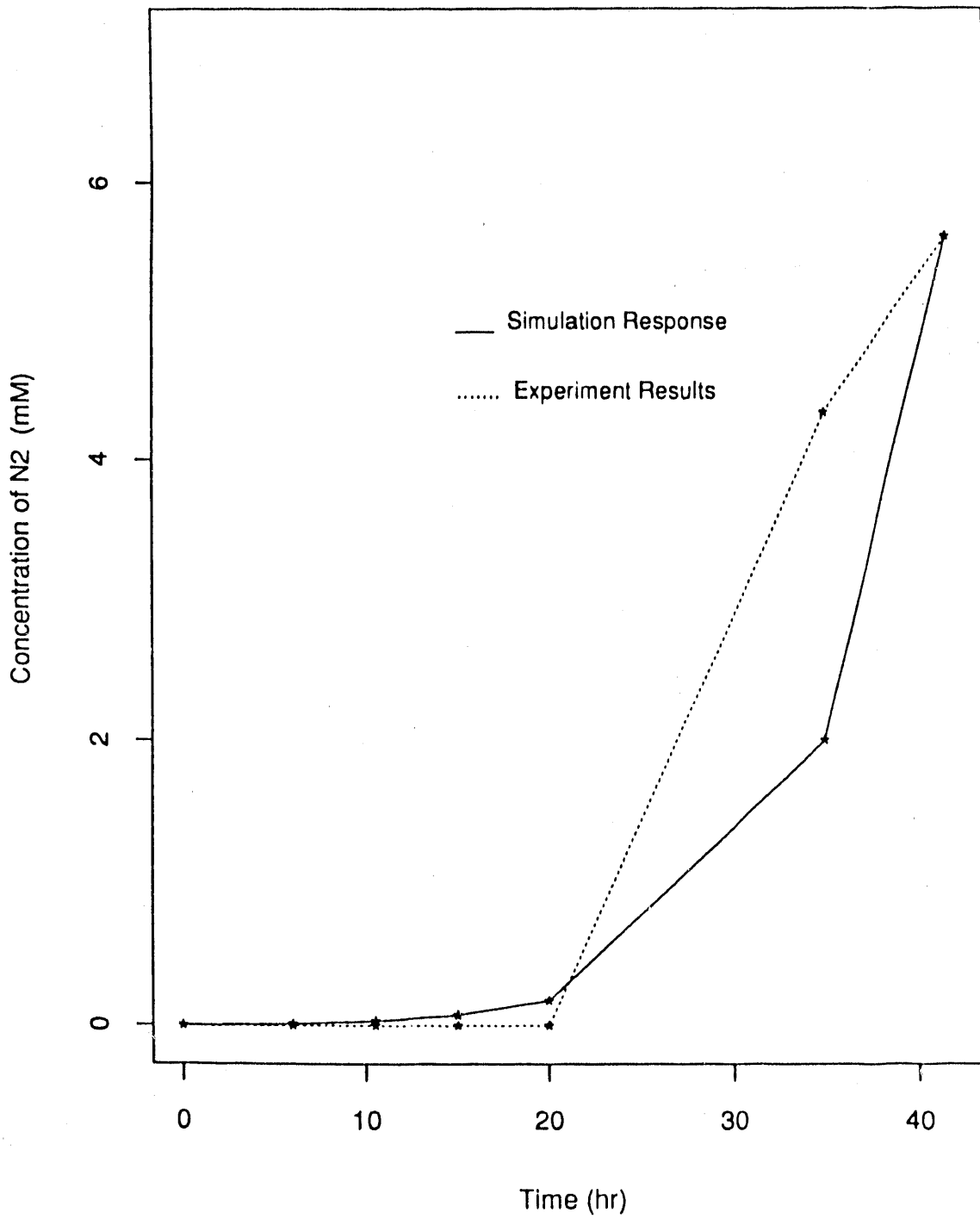during Batch Fermentation

Figure 6.5 : Production of N2
during Batch Fermentation

END

DATE FILMED

01/08/91